The Iranian Journal of Mechanical Engineering Transactions of ISME
Journal homepage: https://jmee.isme.ir/
Vol. 26, No. 2, 2025, pp. 111-134

Research Paper

DOI: https://doi.org/10.30506/jmee.2025.2058190.1373

Analytical Solution for Buckling Analysis of FGM Axisymmetric Cylindrical Shell under Axial Load using Shear Deformation Theory and Perturbation Technique

Mohammad Reza Abbasi[*]
PhD Student

Mehdi Ghannad[†]
Professor

Farid Mahboubi Nasrekani[‡]
Lecture

This paper provides an analytical approach to determining the buckling load of an axisymmetric cylindrical shell made of functionally graded material (FGM) using utilizing the first-order shear deformation theory (FSDT) and von Karman relations. Nonlinear equilibrium equations are derived using the virtual work principle and solved with the perturbation technique. The stability equations are then obtained using the adjacent criterion method, resulting in a system of coupled linear differential equations with variable coefficients, which are solved analytically for the buckling load. A parametric study examines how various geometric and material properties influence the results. It is found that transitioning from homogeneous materials to FGMs increases the buckling load by 4–11%, depending on the shell dimensions. Additionally, finite element method (FEM) results are used to validate the analytical findings and are compared with existing literature.

Keywords: Buckling analysis, Cylindrical shell, Functionally graded materials, Shear deformation theory, Perturbation technique

1 Introduction

Shell buckling analysis is one of the important topics in engineering design. Material properties have a significant effect on the stability and behavior of the shell. The initial concept of

[*]PhD Student, Faculty of Mechanical Engineering, Shahrood University of Technology, Shahrood, Iran, mohammad.reza.abbasi.2011@gmail.com
[†]Corresponding Author, Professor, Faculty of Mechanical Engineering, Shahrood University of Technology, Shahrood, Iran, mghannadk@shahroodut.ac.ir
[‡]Lecture in Mechanical Engineering, School of Engineering, Ulster University, Belfast, UK Correspondence, f.mahboubinasrekani@ulster.ac.uk

Received: 2025/04/19, Revised: 2025/05/24, Accepted: 2025/07/08

functionally graded materials (FGMs) was proposed by Niino et al. in the aerospace organization of Japan, and feasibility studies of FGM production in this country began in 1986 [1]. Using the classical theory of shells, Lorenz determined the buckling load of a thin cylinder under axial load. Von Karman's nonlinear theory was presented in 1941 [2]. Michielsen calculated the buckling of a thin cylindrical shell under axial compression using von Karman and Tsien relations [3]. Nachbar and Hoff determined the buckling of a thin shell with a free edge by classical linear theory [4]. Chen presented buckling and post-buckling of oval cylindrical shells [5]. The critical buckling load of a cylindrical shell made of nickel was determined by Almroth et al. [6]. Hoff and Rehfield obtained a closed-form solution for the classical critical load value of a thin-walled cylindrical shell. For this, they used Donnell's linear equations [7]. Miura introduced a method for the theoretical investigation of isometric buckling deformation of a thin cylindrical shell [8]. The critical load of the thin cylindrical shell was calculated based on the Kirchhoff-Love hypotheses and linearly by Hart-Smith [9]. Feinstein et al. experimentally found the buckling load for oval cylindrical shells with the fixed end [10]. The first-ordeFr shear deformation theory (FSDT) was presented by Reddy and Chandrashekhara, for application in thick shells [2, 11, 12]. Lord et al. obtained a numerical method based on Galerkin spectral decomposition by providing homoclinic solutions in von Karman-Donnell equations [13]. Filippov et al. studied the local buckling of thin-walled square tubes under axial compression in an asymptotic method and compared the results with FEM results [14]. En-Chun and Calladine used a nonlinear FEM and experimental method to investigate the local buckling of thin cylindrical shells [15]. Blandzi and Magnucki investigated the stability of cylindrical shells with invariable and variable axial force [16]. Arjangpay et al. used the meshless local Petrov-Galerkin numerical method (MLPG) to study the buckling of isotropic cylindrical shells under axial load. They obtained displacement field equations based on Donnell and FSDT [17]. Based on the high-order shear deformation theory (HSDT) and analytically, the axially symmetric thick cylinders of FGM with power function of the properties under internal and/or external uniform pressure were investigated by Ghannad and Gharooni, and the results were compared with the results of the FEM [18]. Mahboubi and Eipakchi obtained the elastic buckling of homogeneous and isotropic axisymmetric thin cylindrical shells analytically using the FSDT and used the perturbation technique to solve the equations and compared the results with the FEM and the classical theory [19]. Ghannad et al. analyzed thick cylindrical shells with variable thicknesses of FGM under internal pressure using the FSDT and the perturbation technique and compared the results with the results of the FEM [20]. Duc investigated the nonlinear static and dynamic stability of FGM plates and shells [21]. Shariati et al. performed a numerical analysis of FGM thick-walled cylindrical pressure vessels. For this, they obtained a stiffness matrix from the Galerkin method [22]. Based on the third-order shear deformation theory (TSDT), FGM thick-walled cylinders with the exponential variation of material properties were investigated by Ghannad and Gharooni [23]. Mahboubi and Eipakchi solved the cylindrical shell with variable thickness and axial pressure using the perturbation technique. The displacement field was obtained from the FSDT and von Karman's nonlinear relations, and the governing equations were derived from the virtual work principle [24]. Mahboubi and Eipakchi calculated the buckling load of an axisymmetric nonuniform cylindrical shell with an initial imperfection using the FSDT [25]. Also, they obtained the buckling load of variable thickness cylinders under combined axial and radial loads. They solved the equilibrium equations by perturbation technique and compared the results with FEM results [26]. Sofiyev has conducted a review of research conducted in the field of vibrations and buckling of FGM conical shells. He has presented linear and nonlinear vibration and stability under various loads. The examples of FGM structures included in the review cover [27]. Ifayefunmi et al. investigated the buckling of steel cone-cylinder shells under axial compression and thermal loading numerically and experimentally [28]. Evkin presented a solution using numerical analysis results to investigate the buckling of a cylindrical shell [29]. Li and Kim predicted the ultimate strength of a cylindrical shell with an initial geometrical imperfection

under axial compression with the nonlinear FEM [30]. Recent advances in composite materials, such as carbon nanotube (CNT)-reinforced laminates, have expanded the scope of buckling and vibration analyses. For instance, discrete singular convolution methods have been employed by Civalek and Avcar to study free vibration and buckling of CNT-reinforced non-rectangular plates. This was done using a first-order shear deformation framework and classical theories [31], while cross-ply laminated composites with CNT reinforcements were analyzed for their mechanical stability by Civalek et al. [32]. Ghadimi and Ghannad studied the elastoplastic analysis of axisymmetric thick cylindrical shells subjected to internal pressure with both ends clamped. They utilized shear deformation theories and a radial return mapping method to determine the plastic stress components within the plastic region [33]. Abbasi et al. investigated an analytical solution for buckling analysis of an axisymmetric cylindrical shell made of homogeneous and isotropic materials under axial load using the first-order shear deformation theory [34]. Further extending these analytical approaches, Sofiyev et al. developed a mathematical framework for axially loaded laminated nanocomposite cylindrical shells under axial loading that examines buckling under various environmental conditions within the framework of first-order shear deformation theory [35].

Most researchers used numerical, semi-analytical or experimental methods to determine the buckling load of shells, especially in the nonlinear mode. Some of them have also used analytical methods based on approximate functions such as the Frobenius series. Analytical methods are usually used for linear problems and classical shell theories.

In this paper, an analytical solution to find the buckling load of the axisymmetric cylindrical FGM shell under axial load is presented. The governing equations are derived based on the FSDT with the effect of transverse normal strain and considering the nonlinear kinematic equations of von Karman relations and Hooke's law. Equilibrium equations are systems of coupled nonlinear differential equations with constant coefficients. The stability equations are extracted from the equilibrium equations by the adjacent criterion method and the analytical solution is compared with the FEM. This method is very fast to determine the buckling load for different input data and has very good sensitivity for analysis.

2 Equilibrium equations

A cylindrical shell with length L, middle surface radius R, inner radius r_i, outer radius r_o, and thickness h, is subjected to uniform axial load P. The radial and axial coordinates of a point on the longitudinal section of a symmetrical cylinder are defined by r and x, respectively, and $r = R + z$ where z is measured from the middle surface as shown in Fig. (1).

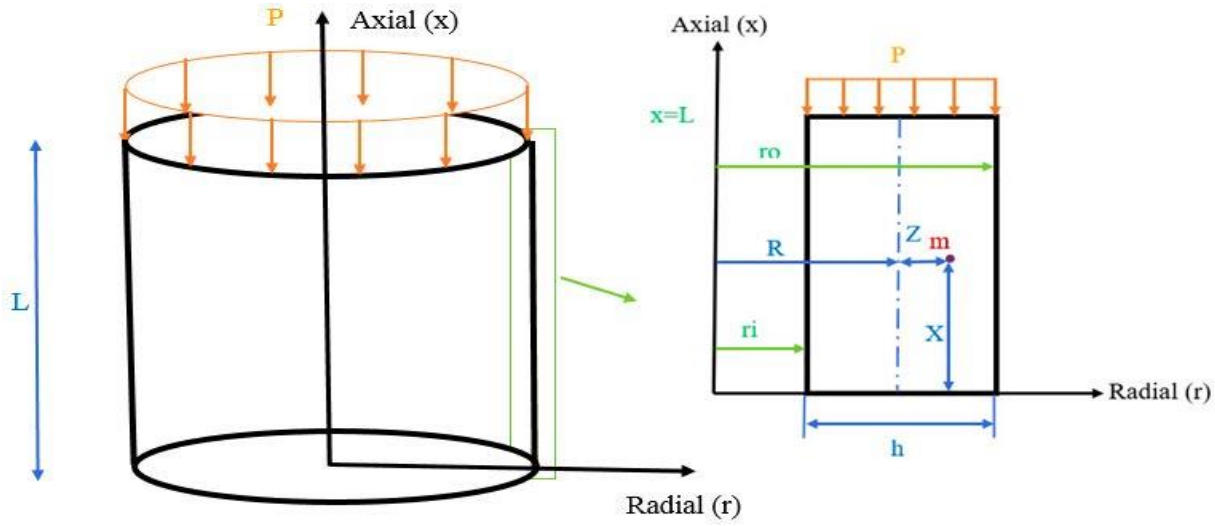

Figure 1 Schematic of the cylindrical shell and its longitudinal section

Using the FSDT for an axisymmetric case, the displacement field is considered as Eqs. (1).

$$\begin{aligned} U_x(x,z) &= u(x) + z\varphi(x) \\ U_z(x,z) &= w(x) + z\psi(x) \\ U_\theta &= 0 \end{aligned} \tag{1}$$

where $U_x(x,z)$, $U_z(x,z)$, and U_θ are axial, radial, and circumferential displacements, respectively. $u(x)$, $w(x)$, $\varphi(x)$, and $\psi(x)$ are unknown functions of x. According to von Karman's nonlinear kinematic relations, strain-displacement relations for large displacements are in the form of Eqs. (2) [12].

$$\varepsilon_x = \frac{\partial U_x}{\partial x} + \frac{1}{2}\left(\frac{\partial U_z}{\partial x}\right)^2;\ \varepsilon_\theta = \frac{U_z}{r};\ \varepsilon_z = \frac{\partial U_z}{\partial z} + \frac{1}{2}\left(\frac{\partial U_z}{\partial z}\right)^2;\ \gamma_{xz} = \frac{\partial U_x}{\partial z} + \frac{\partial U_z}{\partial x} + \frac{\partial U_z}{\partial x}\frac{\partial U_z}{\partial z} \tag{2}$$

where ε_x, ε_z, ε_θ, and γ_{xz} are the axial, radial, circumferential, and shear strains, respectively. The principle of virtual work states $\delta U=\delta W$, where U and W are strain energy and external work, respectively. For an elastic shell, the strain energy and external work done by axial loading are defined as Eqs. (3).

$$\begin{aligned} &U = \iiint \frac{1}{2}\left(\sigma_x\varepsilon_x + \sigma_\theta\varepsilon_\theta + \sigma_z\varepsilon_z + \tau_{xz}\gamma_{xz}\right) r\,d\theta\,dx\,dz \\ &r = R + z; \qquad 0 \le \theta \le 2\pi; \qquad 0 \le x \le L; \qquad -\frac{h}{2} \le z \le \frac{h}{2} \end{aligned} \tag{3a}$$

$$W_p = -\int_{-h/2}^{h/2}\int_0^{2\pi} PU_x\big|_{x=L}\, r\,d\theta\,dz = -2\pi Ph\left(uR + \frac{h^2}{12}\varphi\right) \tag{3b}$$

where σ_x, σ_z, σ_θ, and τ_{xz} are the axial, radial, circumferential, and shear strains, respectively. where P is the load at $x=L$. Heterogeneous FGMs have the same properties in different directions, but their properties are continuously different at any points. The Young's modulus of of FGM in the thick-walled cylindrical shell is assumed in terms of the radial in the form of Eq. (4).

$$E(z) = E_0\left(\frac{R-|z|}{r_i}\right)^n \tag{4}$$

where E_o is the Young's modulus in the inner r_i and outer r_o surfaces of the cylinder, and n is the inhomogeneity constant of the FGM. Poisson's ratio υ varies in a small range for a cylindrical FGM shell. For simplicity, Poisson's ratio is assumed to be constant [19]. According to Hooke's law, stress-strain relations are assumed as the following:

$$\sigma_i = \frac{E(z)}{(1+\upsilon)(1-2\upsilon)}\left[(1-\upsilon)\varepsilon_i + \upsilon(\varepsilon_j + \varepsilon_k)\right];\quad \tau_{xz} = \frac{E(z)}{2(1+\upsilon)}\gamma_{xz} \qquad i \ne j \ne k \tag{5}$$

The stress resultants are defined as follows:

$$\begin{aligned}
&\{N_x, M_x, P_x\} = \int_{-h/2}^{h/2} \{1, z, z^2\} \sigma_x \left(1 + \frac{z}{R}\right) dz; \qquad \{N_\theta, M_\theta\} = \int_{-h/2}^{h/2} \{1, z\} \sigma_\theta dz \\
&\{Q_x, M_{xz}\} = \kappa \int_{-h/2}^{h/2} \{1, z\} \tau_{xz} \left(1 + \frac{z}{R}\right) dz; \qquad N_z = \int_{-h/2}^{h/2} \sigma_z \left(1 + \frac{z}{R}\right) dz
\end{aligned} \tag{6}$$

where κ is the shear correction factor, and it is considered 5/6 in this study. Equilibrium equations and boundary conditions as functions of the stress resultants are derived by applying the principle of virtual work as the follows:

$$\begin{aligned}
&eq1: R\frac{dN_x}{dx} = 0 \\
&eq2: R\frac{dM_x}{dx} - RQ_x = 0 \\
&eq3: R\frac{d}{dx}\left(N_x \frac{dw}{dx} + M_x \frac{d\psi}{dx} + Q_x(1+\psi)\right) - N_\theta = 0 \\
&eq4: R\frac{d}{dx}\left(N_x \frac{dw}{dx} + P_x \frac{d\psi}{dx} + M_{xz}\right) - M_\theta - RN_z(1+\psi) - RQ_x \frac{dw}{dx} + R\psi \frac{dM_{xz}}{dx} = 0
\end{aligned} \tag{7a}$$

$$\begin{aligned}
&\left(R(N_x + Ph)\delta u\right)\Big|_{x=L} - \left(RN_x \delta u\right)\Big|_{x=0} = 0 \\
&\left(R\left(M_x + \frac{Ph^3}{12}\right)\delta\varphi\right)\Big|_{x=L} - \left(RM_x \delta\varphi\right)\Big|_{x=0} = 0 \\
&\left(R\left(N_x \frac{dw}{dx} + M_x \frac{d\psi}{dx} + Q_x(1+\psi)\right)\delta w\right)\Big|_{x=0}^{x=L} = 0 \\
&\left(R\left(M_x \frac{dw}{dx} + P\frac{d\psi}{dx} + M_{xz}(1+\psi)\right)\delta\psi\right)\Big|_{x=0}^{x=L} = 0
\end{aligned} \tag{7b}$$

From the first boundary condition of Eqs. (7b), Eq. (8) can be deduced.

$$N_x = -Ph \text{ at } x = L \tag{8}$$

In other words, the stress resultant N_x is constant. The equilibrium equations (Eqs. (7a)) include four coupled nonlinear differential equations with constant coefficients. By substituting Eqs. (1-6) into Eqs. (7), the governing equations as functions of displacements are determined and their dimensionless form has been reported later. To solve these equations, it is necessary to transform them into a dimensionless form. For this aim, the dimensionless parameters are defined as follows:

$$\begin{aligned}
&x^* = \frac{x}{L}; h^* = \frac{h}{h_0}; R^* = \frac{R}{r_0}; r_i^* = \frac{r_i}{r_0}; z^* = \frac{r_0}{h_0}; u^* = \frac{u}{h_0}; w^* = \frac{w}{h_0}; \epsilon = \frac{h_0}{L} \\
&E^* = \frac{E}{E_0}; P^* = \frac{P}{\varepsilon E_0}; V = \epsilon \frac{du^*}{dx^*}; m_1 = \ln\left(\frac{2R-h}{R}\right); m_2 = \ln\left(\frac{2R-h}{2R}\right); m_3 = \ln\left(\frac{2R+h}{R}\right)
\end{aligned} \tag{9}$$

In the above relation, r_0 and h_0 are the radius and thickness characteristics, respectively. L is the shell length, superscript (*) stands for a dimensionless parameter, and ϵ is a dimensionless small perturbation parameter. By using the above dimensionless parameters and applying them to the equilibrium Eqs. (7) and integrating from the first equation and considering the new variable $X=x^*/\epsilon$, the dimensionless form of the equations is extracted. These equations are reported in Appendix (1). To solve these equations, a straightforward expansion method of the perturbation technique has been used [36]. The solution is considered as the following uniform series:

$$\begin{aligned} V^* &= \epsilon V_0^* + \epsilon^2 V_1^*; \qquad \varphi = \epsilon\varphi_0 + \epsilon^2\varphi_1 \\ W^* &= \epsilon W_0^* + \epsilon^2 W_1^*; \qquad \psi = \epsilon\psi_0 + \epsilon^2\psi_1 \end{aligned} \tag{10}$$

By replacing Eqs. (10) into the dimensionless form of equations and considering terms with the same order of ϵ, the zero and first-order equations are determined as Eqs. (11). These equations are a system of four coupled linear nonhomogeneous equations and their total solution is the summation of the general and particular solutions.

$$\text{zero- order: } [A_2]\frac{d^2\{Y_0\}}{dX^2}+[A_1]\frac{d\{Y_0\}}{dX}+[A_0]\{Y_0\}=\{F_0\}; \qquad \{Y_0\}=\begin{Bmatrix} V_0^* & \varphi_0 & w_0^* & \psi_0 \end{Bmatrix} \tag{11a}$$

$$\text{first- order: } [A_2]\frac{d^2\{Y_1\}}{dX^2}+[A_1]\frac{d\{Y_1\}}{dX}+[A_0]\{Y_1\}=\{F_1\}; \qquad \{Y_1\}=\begin{Bmatrix} V_1^* & \varphi_1 & w_1^* & \psi_1 \end{Bmatrix} \tag{11b}$$

The matrices $[A_0]$, $[A_1]$, and $[A_2]$, vectors $\{F_0\}$ and $\{F_1\}$ are reported in Appendix (2). The general solution of zero-order equations (Eq. (11a)) is considered as $\{Y_0\}_g = \{V\}\exp(\lambda X)$, where λ is the eigenvalue and $\{V\}$ is the corresponding eigenvector. The general solution is obtained in the form of Eq. (12).

$$\{Y_0\}_g = \sum_{i=1}^{6} C_i \{V_i\} \exp(\lambda_i X) \tag{12}$$

where C_i are the constant coefficients of the general solution. The particular solution for the zero-order equations is determined as follows:

$$\{Y_0\}_p = [A_0]^{-1}\{F\} \tag{13}$$

The total solution of zero-order equations is in the form of Eq. (14).

$$\{Y_0\} = \{Y_0\}_g + \{Y_0\}_p \tag{14}$$

By calculating $V_0{}^*$, $u_0{}^*$ is obtained through Eq. (15).

$$u_0^* = \int V_0^* dx^* + C_7 \tag{15}$$

By placing the boundary conditions, the coefficients C_i and, accordingly, u_0^*, φ_0, w_0^*, and ψ_0 are determined. By substituting the zero-order solution them in the first-order equations (Eq. (11b)), these equations are solved. Since the homogeneous parts of these equations are the same, the general solution of them is the same as Eq. (12). Non-homogeneous components of first-order equations include exponential and polynomial expressions which are functions of $\{Y_0\}$ components. The particular solution related to the polynomial part is considered as Eq. (16).

$$\{Y_1\}_{p1} = \{B_1\} X + \{B_0\} \tag{16}$$

The particular solution of the exponential part is in the form of Eq. (17).

$$\{Y_1\}_{p2} = \sum_i \left(\{C_2\}_i X^2 + \{C_1\}_i X + \{C_0\}_i\right) \exp\left(\lambda_i X\right) + \sum_j \{D\}_j \exp\left(n_j X\right) \tag{17}$$

where λ_i is eigenvalues of the general solution and n_j is the exponential coefficient of the heterogeneous terms.. The constant coefficient vectors $\{B_1\}$, $\{B_0\}$, $\{C_2\}$, $\{C_1\}$, $\{C_0\}$, and $\{D\}$ are determined by substituting Eqs. (16, 17) into Eq. (11b). The general solution of first-order equations is determined as follows:

$$\{Y_1\} = \{Y_1\}_g + \{Y_1\}_{p1} + \{Y_1\}_{p2} \tag{18}$$

By calculating V_1^*, u_1^* is obtained similar to Eq. (15). By applying the boundary conditions in the general solution, the values of coefficients C_i are obtained and the expressions u_1^*, φ_1, w_1^*, and ψ_1 are determined. Using Eqs. (10), the solution of the equilibrium equations (V^*, φ, w^*, and ψ) is extracted.

3 Stability equations

To derive the stability equations, the adjacent criterion method is used. According to this method, the stability equations are derived using the equilibrium equations and their solution which are explained in the previous section. For this aim, the displacements and their increments are considered as follows [2]:

$$V^* = V_e^* + V_s^*; \qquad \varphi = \varphi_e + \varphi_s; \qquad w^* = w_e^* + w_s^*; \qquad \psi = \psi_e + \psi_s \tag{19}$$

where the parameters with subscript *e* represent a moment before buckling and in the equilibrium state, and they satisfy the equilibrium equations, and the parameters with subscript *s* represent small increments after buckling. By inserting the above relations into the equilibrium equations and by removing the nonlinear terms due to their smallness, stability equations are derived, and they are reported in Appendix (3). These equations are a system of coupled linear homogeneous differential equations with variable coefficients and they can be shown in the following matrix form:

$$[B_2]\frac{d^2\{Y_s\}}{dX^2} + [B_1]\frac{d\{Y_s\}}{dX} + [B_0]\{Y_s\} = \{0\}; \qquad \{Y_s\} = \begin{Bmatrix} V_s^* & \varphi_s & w_s^* & \psi_s \end{Bmatrix}^T \tag{20}$$

where $[B_0]$, $[B_1]$, and $[B_2]$ are the matrices of coefficients in the equations. These matrices are variable and are replaced by their average value. To determine the general solution of Eq. (20), the solution is considered as follows:

$$\{Y_s\} = \{V\}\exp(\alpha X) \tag{21}$$

where $\{V\}$ is eigenvector and α is eigenvalue. By placing this solution, the system of algebraic Eq. (22) is extracted.

$$[ax] = [B_2]\alpha^2 + [B_1]\alpha + [B_0] \tag{22}$$

By setting the determinant of this equation equal to zero, the characteristic equation is obtained. The roots of this equation are eigenvalues, and they are functions of P_{cr}^*. For each eigenvalue, there is a corresponding eigenvector. The general solution is considered as follows:

$$\{Y_s\} = \sum_{i=1}^{6} C_i \{V\}_i \exp(\alpha_i X) \tag{23}$$

By applying the boundary conditions a system of algebraic equations is derived as follows:

$$[bx]_{6\times6}\{C_1, C_2, C_3, C_4, C_5, C_6\} = \{0\}_{6\times1} \tag{24}$$

where the components of the matrix [*bx*] are functions of P_{cr}^* and α. By setting the determinant [*bx*] equal to zero, an equation is obtained, which is a complex algebraic function in terms of P_{cr}^*. The root of this equation is the buckling load, which is obtained by using the bisection method and considering the boundary conditions.

4 Numerical solution

DS SIMULIA Suite 2022 software (Abaqus/CAE 2022) was used to determine the buckling load of the FGM cylindrical shell. CAX8 is used to analyze the eight-node axisymmetric quadrilateral element. The mesh size was chosen by trial and error to eliminate the sensitivity of the results to changes in the mesh size. The boundary conditions of the shell are fixed at X=0 and movement along the axis is free at X=1. USDFLD subroutine of Abaqus software is used to define FGM properties. Shell parameters are listed in Table (1).

Table 1 Shell specifications

Parameters	Value
Length	$L = 0.2\ 3$
Inner radius	$r_i = 0.05\ m$
Outer radius	$r_o = 0.06\ m$
Poisson's ratio	$\upsilon = 0.3$
Young's modulus in the inner and outer radius	$E_o = 200\ GPa$

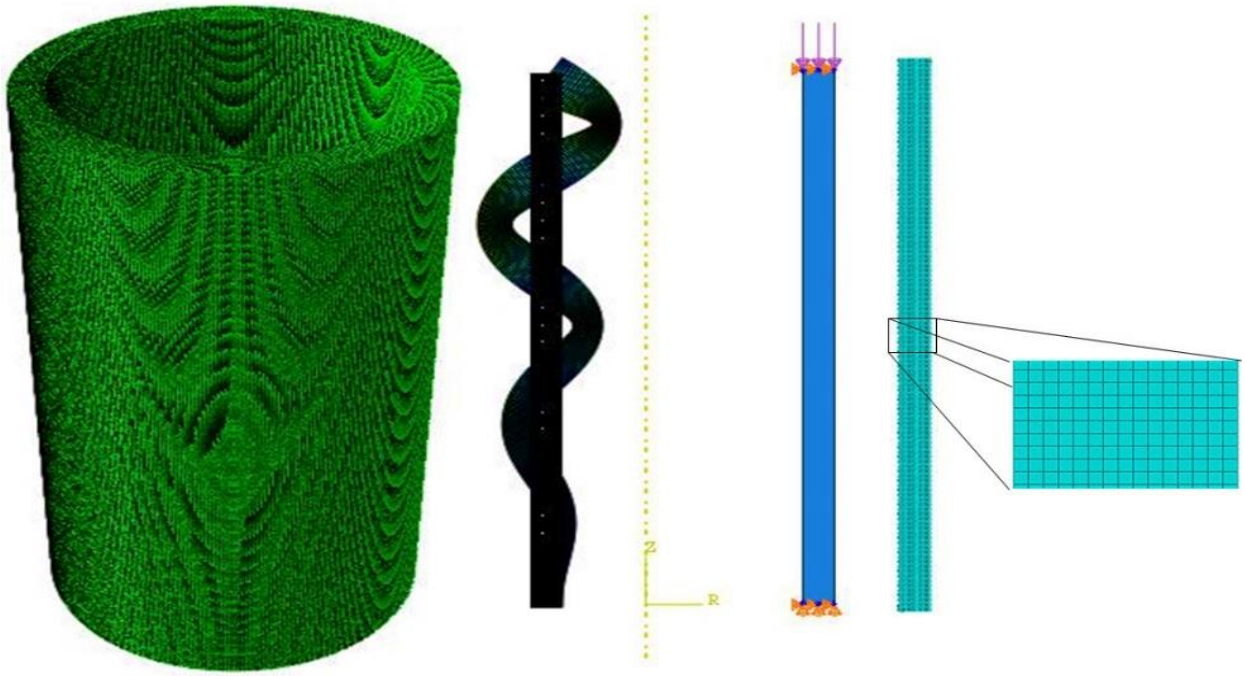

Figure 2 Mesh pattern, loading, boundary conditions, and buckled shell

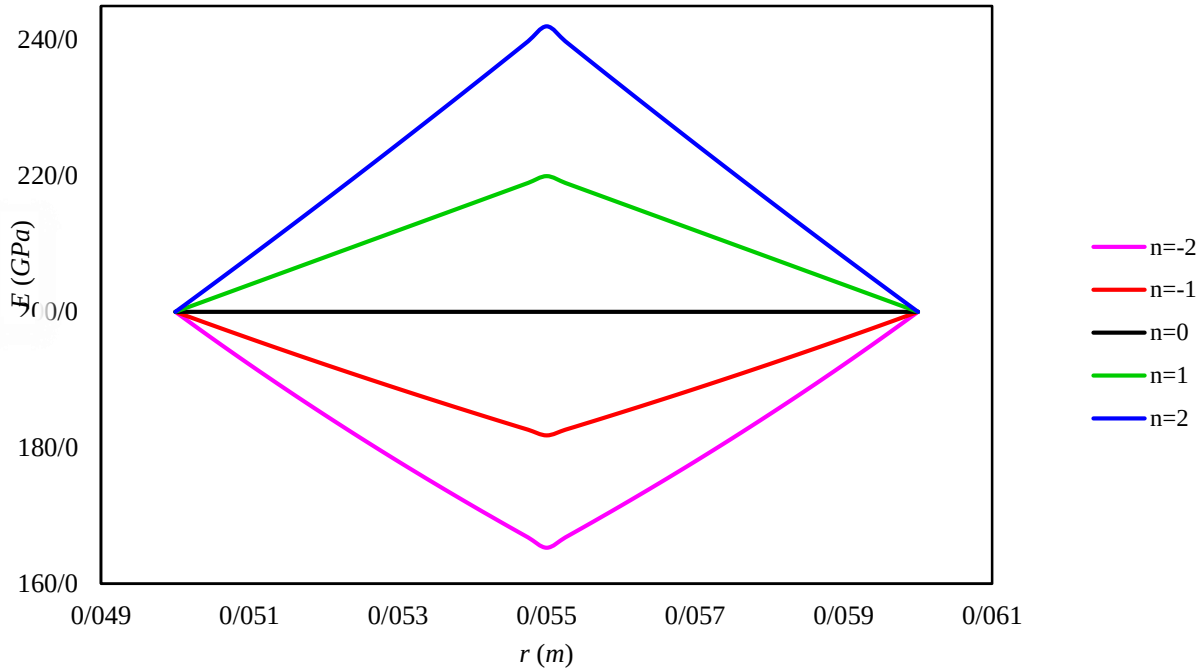

Figure 3 Changes in modulus of elasticity in terms of radius

The changes of Young's modulus in terms of radius for different values of n are shown in Fig. (3).

5 Discussion and results

According to the analytical procedure, the buckling load of the FGM cylindrical shell has been determined, and a program has been prepared to perform calculations using Maple 2015 software. First, the accuracy of the solution was checked. In all cases, the modulus of elasticity and Poisson's ratio are $E_o = 200\ GPa$ and $\upsilon = 0.3$, respectively.

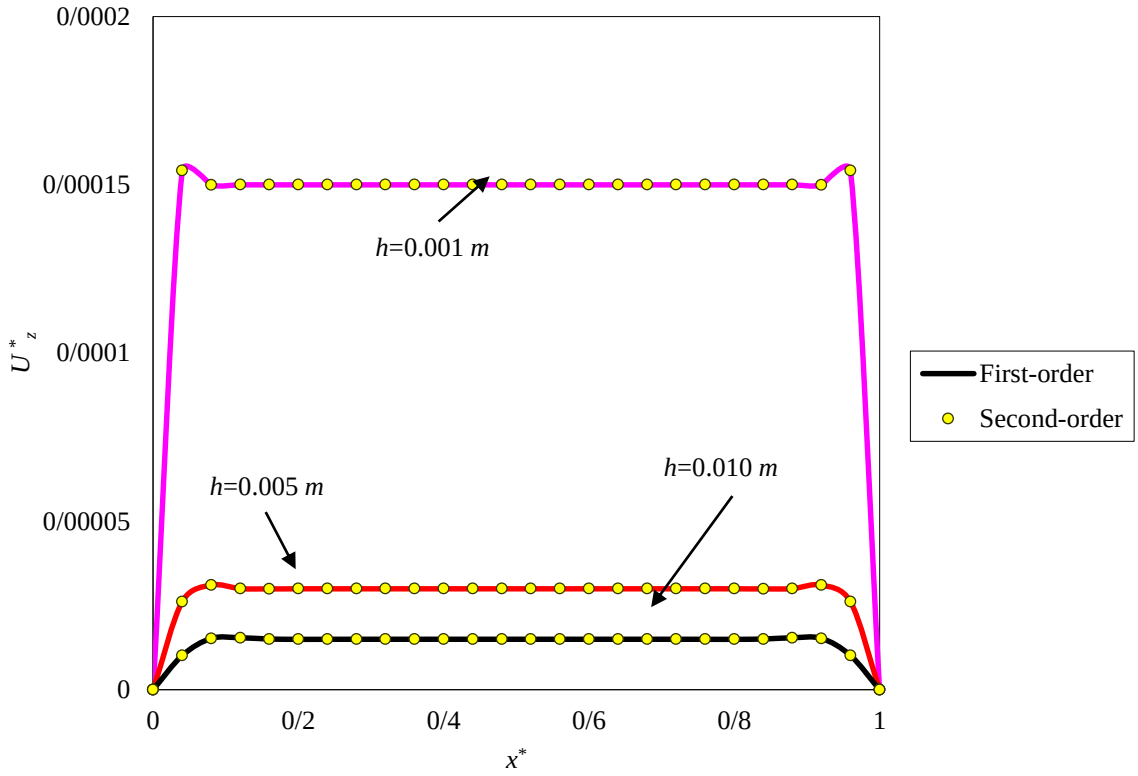

Figure 4 Comparison of analytical first and second-order radial dimensionless displacement of homogeneous shells (P=1 MPa, L=0.8 m, R=0.1 m, $z = \pm h/2$)

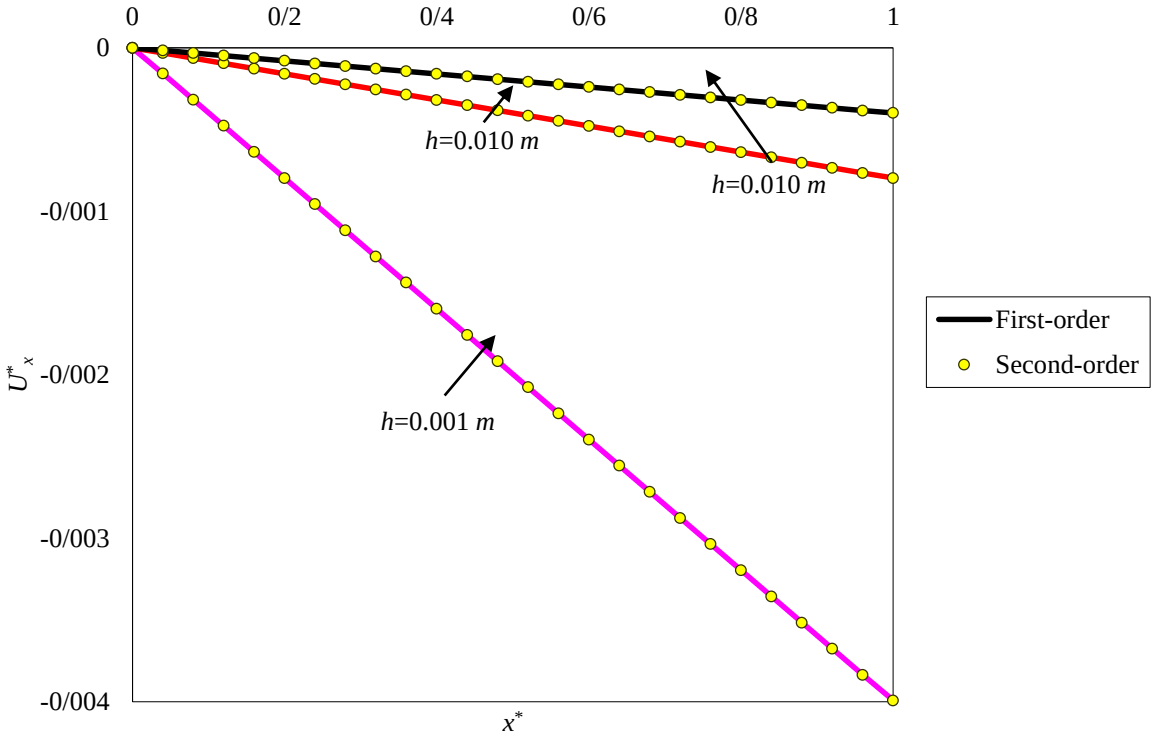

Figure 5 Comparison of analytical first and second-order axial dimensionless displacement of homogeneous shells (P=1 MPa, L=0.8 m, R=0.1 m, $z = \pm h/2$)

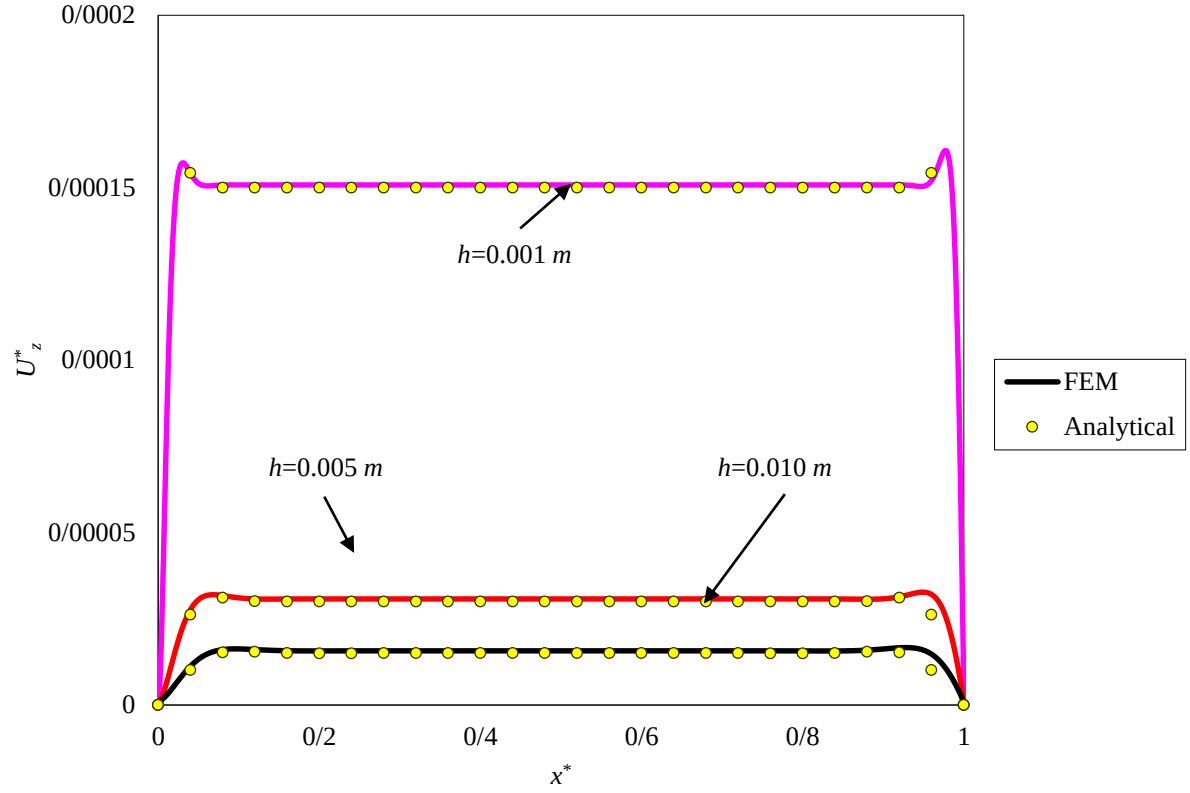

Figure 6 Comparison of numerical and analytical second-order radial dimensionless displacement of homogeneous shells (P=1 MPa, L=0.8 m, R=0.1 m, $z = \pm h/2$)

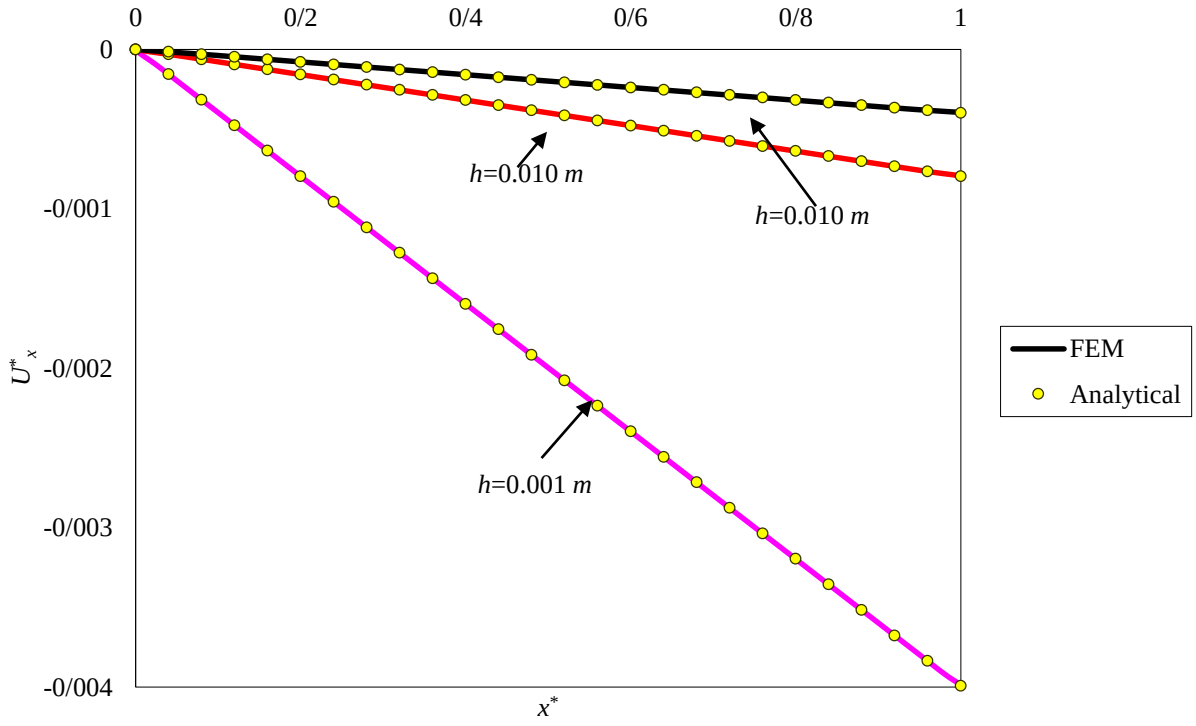

Figure 7 Comparison of numerical and analytical second-order axial dimensionless displacement of homogeneous shells (P=1 MPa, L=0.8 m, R=0.1 m, $z = \pm h/2$)

According to the Eqs. (1), (10), and (15), in Figs. (4) and (5) the dimensionless displacements of the first-order and second-order approximations, respectively, radially and axially, and in Figs. (6) and (7), the dimensionless displacements of the FEM and the second-order analytical method in the inner or outer wall if the cylinder, respectively, radially and axially, in terms of the dimensionless variable x^*, with different thicknesses h. The second order is appropriate for this study and other results are reported in this order. Also, the results of solving equilibrium equations by analytical method and FEM are in good agreement with each other. In addition, the radial displacement is very small compared to the axial displacement.
In Table (2), the buckling load of homogeneous shells (n=0) with constant thickness is reported, and they are compared with the results [19] and the classical theory [37] for different thicknesses h have been compared. In the classical theory, the buckling load is obtained from Eq. (25). It can be seen that the analysis solution results are in good agreement with the FEM and the introduced references. As stated in section 4, the axially symmetric mode has been used in the FEM solution; This issue can cause a slight difference between the results of the solution and the results of the three-dimensional FEM results [19].

$$P_{cr} = 0.605\frac{Eh}{R} \tag{25}$$

To generalize the results, the critical load is defined in dimensionless form through Eqs. (9). In Table (3), the dimensionless buckling load of homogeneous shells (n=0) with constant thickness and different lengths L obtained from analytical, finite element, and classical methods are shown. It can be seen that the analytical solution results are in good agreement with the FEM. Also, with the increase in length, the difference between the results of classical theory and analytical methods and FEM increases.

Table 2 Comparison of analytical and numerical buckling load (MPa) of homogeneous shells (L=0.8 m, R=0.1 m)

	Recent study		Ref. [19]	Ref. [37]
h (m)	FSDT	FEM	Analytical	Classical theory
0.001	1.20e03	1.21e3	1.21e3	1.21e3
0.005	6.44e03	5.97e3	5.26e3	6.05e3
0.01	1.14e4	1.18e4	1.006e4	1.21e4

Table 3 Comparison of analytical, numerical, and classical dimensionless buckling load of homogeneous shells (h=0.01 m, R=0.055 m)

L (m)	FEM	FSDT	Classical theory
0.12	1.3005	1.3158	1.3200
0.16	1.7089	1.7361	1.7600
0.2	2.1220	2.1584	2.2000
0.24	2.5375	2.5794	2.6400
0.28	2.9543	3.0008	3.0800

Table (4) shows the effect of L length changes on the dimensionless buckling load calculated by numerical and analytical methods. In the studied range of parameters, as the length decreases by approximately 57%, the dimensionless buckling load decreases by approximately 56%. As n changes from -2 to 2, the dimensionless buckling load increases by about 10%. It can be seen that the dimensionless buckling load can be increased by about 5% using FGM (n=2) compared to the homogeneous material (n=0). As n increases, the difference between the analytical solution and the FEM increases slightly.
In Table (6), the effect of changes in thickness h on the dimensionless buckling load calculated by numerical and analytical methods is presented. In the studied range of parameters, an approximately 133% increase in thickness decreases the dimensionless buckling load by approximately 8%.

Table 4 Effect of length changes on dimensionless buckling load of numerical and analytical solution (h=0.01 m, R=0.055 m)

L (m)	Method	$n=-2$	$n=-1$	$n=0$	$n=1$	$n=2$
0.12	FEM	1.2934	1.2969	1.3005	1.3043	1.3083
	FSDT	1.2546	1.2848	1.3158	1.3475	1.3801
0.16	FEM	1.6995	1.7041	1.7089	1.7139	1.7192
	FSDT	1.6538	1.6944	1.7361	1.7788	1.8225
0.20	FEM	2.1103	2.1160	2.1220	2.1283	2.1349
	FSDT	2.0558	2.1065	2.1584	2.2117	2.2664
0.24	FEM	2.5235	2.5303	2.5375	2.5450	2.5529
	FSDT	2.4562	2.5170	2.5794	2.6434	2.7090
0.28	FEM	2.9380	2.9460	2.9543	2.9631	2.9723
	FSDT	2.8571	2.9280	3.0008	3.0755	3.1521

Table 5 Effect of radius changes on the dimensionless buckling load of numerical and analytical solution (h=0.01 m, L=0.20 m)

R (m)	Method	$n=-2$	$n=-1$	$n=0$	$n=1$	$n=2$
0.035	FEM	3.2085	3.2225	3.2377	3.2540	3.2716
	FSDT	3.0909	3.2748	3.4232	3.6344	3.8144
0.045	FEM	2.5452	2.5537	2.5627	2.5722	2.5824
	FSDT	2.6125	2.6750	2.7040	2.8350	2.9790
0.055	FEM	2.1103	2.1160	2.1220	2.1283	2.1349
	FSDT	2.0558	2.1065	2.1584	2.2117	2.2664
0.065	FEM	1.8074	1.8115	1.8157	1.8202	1.8248
	FSDT	1.8955	1.8896	1.9633	2.0114	2.0769
0.075	FEM	1.5788	1.5819	1.5851	1.5884	1.5918
	FSDT	1.6222	1.6655	1.7104	1.7571	1.8056

Table 6 Effect of thickness changes on the dimensionless buckling load of numerical and analytical solution (L=0.20 m, R=0.055 m)

h (m)	Method	$n=-2$	$n=-1$	$n=0$	$n=1$	$n=2$
0.006	FEM	2.1473	2.1507	2.1543	2.1579	2.1617
	FSDT	2.2445	2.2929	2.3579	2.3943	2.4473
0.008	FEM	2.1299	2.1345	2.1392	2.1442	2.1493
	FSDT	2.2125	2.2378	2.3042	2.3734	2.4611
0.010	FEM	2.1103	2.1160	2.1220	2.1283	2.1349
	FSDT	2.0558	2.1065	2.1584	2.2117	2.2664
0.012	FEM	2.0946	2.1014	2.1086	2.1163	2.1245
	FSDT	2.1189	2.2205	2.2358	2.3314	2.4511
0.014	FEM	2.0767	2.0847	2.0932	2.1024	2.1122
	FSDT	2.1049	2.1067	2.2281	2.3576	2.4445

As n changes from -2 to 2, the dimensionless buckling load increases by about 9-16%. It can be seen that the dimensionless buckling load can be increased by 4-10% using FGM (n=2) compared to homogeneous material (n=0). As n increases, the difference between the analytical solution and the FEM increases. It can be seen that the proposed method is in good agreement with the FEM results, even for thick shells. As the thickness increases, the sensitivity to n changes increases.

6 Conclusion

An analytical solution was proposed to find the buckling load of an axisymmetric FGM cylindrical shell with constant thickness under axial load. The governing equations were derived using the FSDT and von Karman relations. In this study, the equilibrium equations, which are coupled nonlinear differential equations, were solved using the perturbation technique. The stability equations, which are a system of coupled linear differential equations with variable coefficients, were solved analytically and the critical load was obtained. By conducting a parametric study, the effect of changing the geometric and mechanical properties of the shell on the buckling load was investigated. By decreasing the radius or increasing the thickness, the sensitivity to n changes increases. This analytical solution has fast convergence and good accuracy. Obtaining the buckling load with the presented method is easier and faster than the FEM because it does not need to create the FEM model and its meshing.

References

[1] M. Koizumi, and M. Niino, "Overview of FGM Research in Japan", *MRS Bulletin,* Vol. 20, No. 1, pp. 19-21, 1995, https://doi.org/10.1557/S0883769400048867.

[2] D. O. Brush, B. O. Almroth, and J. Hutchinson, "*Buckling of Bars, Plates, and Shells"*, New York, McGraw-Hill, Vol. 42, No. 4, pp. 911, 1975, https://doi.org/10.1115/1.3423754.

[3] H. F. Michielsen, "The Behavior of Thin Cylindrical Shells after Buckling under Axial Compression", *Journal of the Aeronautical Sciences*, Vol. 15, No. 12, pp. 738-744, 1948, https://doi.org/10.2514/8.11706.

[4] W. Nachbar, and N. J. Hoff, "The Buckling of a Free Edge of an Axially-compressed Circular Cylindrical Shell", *Quarterly of Applied Mathematics*, Vol. 20, No. 3, pp. 267-277, 1962, https://doi.org/10.1090/qam/140215.

[5] Y.-N. Chen, "*Buckling and Postbuckling of an Oval Cylindrical Shell under Axial Compression"*, Ph.D. Theses, Polytechnic University ProQuest Dissertations & Theses, Brooklyn, Polytechnic University, 1964.

[6] B. O. Almroth, A. M. Holmes, and D. O. Brush, "An Experimental Study of the Bucking of Cylinders under Axial Compression: Test Program is Aimed at Determining the Causes of Discrepancy between Theoretical and Experimental Results for the Buckling Load of Axially Compressed Cylindrical Shells", *Experimental Mechanics*, Vol. 4, No. 9, pp. 263-270, 1964, https://doi.org/10.1007/BF02323088.

[7] N. J. Hoff, and L. W. Rehfield, "Buckling of Axially Compressed Circular Cylindrical Shells at Stresses Smaller than the Classical Critical Value", *Journal of Applied Mechanics*, Vol. 32, No. 3, pp. 542-546, 1965, https://doi.org/10.1115/1.3627256.

[8] K. Miura, "Inextensional Buckling Deformations of General Cylindrical Shells", *AIAA Journal*, Vol. 6, No. 5, pp. 966-968, 1968, https://doi.org/10.2514/3.4651.

[9] L. Hart-Smith, "Buckling of Thin Cylindrical Shells under Uniform Axial Compression", *International Journal of Mechanical Sciences*, Vol. 12, No. 4, pp. 299-313, 1970, https://doi.org/10.1016/0020-7403(70)90084-6.

[10] G. Feinstein, B. Erickson, and J. Kempner, "Stability of Oval Cylindrical Shells: Experimental Investigation of Initial and Ultimate Buckling Loads of Fixed-End, Oval Cylindrical Shells under Axial Compression", *Experimental Mechanics*, Vol. 11, pp. 514-520, 1971, https://doi.org/10.1007/BF02327691.

[11] C. R. Calladine, *Theory of Shell Structures*, New York, Cambridge University Press, 1989.

[12] M. Amabili, *Nonlinear Vibrations and Stability of Shells and Plates*, Cambridge, Cambridge University Press, 2008, Nonlinear Vibrations and Stability of Shells and Plates - Marco Amabili - Google Books.

[13] G. J. Lord, A. R. Champneys, and G. W. Hunt, "Computation of Homoclinic Orbits in Partial Differential Equations: An Application to Cylindrical Shell Buckling", *SIAM Journal on Scientific Computing*, Vol. 21, No. 2, pp. 591-619, 1999, https://doi.org/10.1137/S1064827597321647.

[14] S. Filippov, E. Haseganu, and A. Smirnov, "Buckling Analysis of Axially Compressed Square Elastic Tubes with Weakly Supported Edges", *Technische Mechanik*, Vol. 20, No. 1, pp. 13-20, 2000, https://journals.ub.ovgu.de/index.php/techmech/article/view/1067.

[15] Z. En-chun, and C. R. Calladine, "Buckling of Thin Cylindrical Shells under Locally Axial Compression", *Engineering Mechanics*, Vol. 20, No. 2, pp. 168-170, 2003, https://engineeringmechanics.cn/en/article/id/3739.

[16] E. Magnucka-Blandzi, and K. Magnucki, "Elastic Buckling of an Axially Compressed Open Circular Cylindrical Shell", *Proceedings in Applied Mathematics and Mechanics*, Vol. 4, No. 1, pp. 546-547, 2004, https://doi.org/10.1002/pamm.200410254.

[17] A. Arjangpay, M. Darvizeh, R. Ansari, and G. Zarepour, "Axial Buckling Analysis of an Isotropic Cylindrical Shell using the Meshless Local Petrov-Galerkin Method", *Computational Methods in Civil Engineering*, Vol. 2, No. 2, pp. 219-230, 2011, https://cmce.guilan.ac.ir/article_903_0.html.

[18] M. Ghannad, and H. Gharooni, "Displacements and Stresses in Pressurized Thick FGM Cylinders with Varying Properties of Power Function Based on HSDT", *Journal of Solid Mechanics*, Vol. 4, No. 3, pp. 237-251, 2012, https://journals.iau.ir/article_514480.html.

[19] F. Mahboubi Nasrekani, and H. R. Eipakchi, "Elastic Buckling of Axisymmetric Cylindrical Shells under Axial Load using First Order Shear Deformation Theory", *ZAMM-Journal of Applied Mathematics and Mechanics*, Vol. 92, No. 11-12, pp. 937-944, 2012, https://doi.org/10.1002/zamm.201200004.

[20] M. Ghannad, G. H. Rahimi, and M. Z. Nejad, "Elastic Analysis of Pressurized Thick Cylindrical Shells with Variable Thickness Made of Functionally Graded Materials", *Composites Part B: Engineering*, Vol. 45, No. 1, pp. 388-396, 2013, https://doi.org/10.1016/j.compositesb.2012.09.043.

[21] N. D. Duc, *Nonlinear Static and Dynamic Stability of Functionally Graded Plates and Shells*. Hanoi, Vietnam National University Press, 2014.

[22] M. Shariati, H. Sadeghi, M. Ghannad, and H. Gharooni, "Semi Analytical Analysis of FGM Thick-walled Cylindrical Pressure Vessel with Longitudinal Variation of Elastic Modulus under Internal Pressure", *Journal of Solid Mechanics*, Vol. 7, No. 2, pp. 131-145, 2015, https://journals.iau.ir/article_514636.html.

[23] M. Ghannad, and H. Gharooni, "Elastic Analysis of Pressurized Thick FGM Cylinders with Exponential Variation of Material Properties using TSDT", *Latin American Journal of Solids and Structures*, Vol. 12, No. 6, pp. 1024-1041, 2015, https://doi.org/10.1590/1679-78251491.

[24] F. Mahboubi Nasrekani, and H. R. Eipakchi, "An Analytical Procedure for Buckling Load Determination of an Axisymmetric Cylinder with Non-uniform Thickness using Shear Deformation Theory", *AUT Journal of Mechanical Engineering*, Vol. 1, No. 2, pp. 211-218, 2017, https://doi.org/10.22060/mej.2017.12557.5364.

[25] F. Mahboubi Nasrekani, and H. R. Eipakchi, "Axisymmetric Buckling of Cylindrical Shells with Nonuniform Thickness and Initial Imperfection", *International Journal of Steel Structures*, Vol. 19, pp. 435-445, 2019, https://doi.org/10.1007/s13296-018-0132-9.

[26] F. Mahboubi Nasrekani, and H. R. Eipakchi, "Analytical Solution for Buckling Analysis of Cylinders with Varying Thickness Subjected to Combined Axial and Radial Loads", *International Journal of Pressure Vessels and Piping*, Vol. 172, pp. 220-226, 2019, https://doi.org/10.1016/j.ijpvp.2019.03.036.

[27] A. Sofiyev, "Review of Research on the Vibration and Buckling of the FGM Conical Shells," *Composite Structures*, Vol. 211, pp. 301-317, 2019, https://doi.org/10.1016/j.compstruct.2018.12.047.

[28] O. Ifayefunmi, M. Ismail, and M. Othman, "Buckling of Unstiffened Cone-Cylinder Shells Subjected to Axial Compression and Thermal Loading", *Ocean Engineering*, Vol. 225, p. 108601, 2021, https://doi.org/10.1016/j.oceaneng.2021.108601.

[29] A. Evkin, "Analytical Model of Local Buckling of Axially Compressed Cylindrical Shells", *Thin-Walled Structures*, Vol. 168, pp. 108261, 2021, https://doi.org/10.1016/j.tws.2021.108261.

[30] S. Li, and D. K. Kim, "Ultimate Strength Characteristics of Unstiffened Cylindrical Shell in Axial Compression," *Ocean Engineering*, Vol. 243, pp. 110253, 2022, https://doi.org/10.1016/j.oceaneng.2021.110253.

[31] Ö. Civalek, and M. Avcar, "Free Vibration and Buckling Analyses of CNT Reinforced Laminated Non-rectangular Plates by Discrete Singular Convolution Method," *Engineering with Computers*, Vol. 38, No. Suppl 1, pp. 489-521, 2022, https://doi.org/10.1007/s00366-020-01168-8.

[32] Ö. Civalek, S. Dastjerdi, and B. Akgöz, "Buckling and Free Vibrations of CNT-Reinforced Cross-Ply Laminated Composite Plates," *Mechanics Based Design of Structures and Machines*, Vol. 50, No. 6, pp. 1914-1931, 2022, https://doi.org/10.1080/15397734.2020.1766494.

[33] M. Ghadimi, and M. Ghannad, "Elasto-plastic Analysis of Thick Cylinders using Shear Deformation Theories and Radial Return Mapping Method", *Iranian Journal of Mechanical Engineering Transactions of the ISME*, Vol. 25, No. 2, 2024, https://doi.org/10.30506/jmee.2024.2023842.1342.

[34] M. R. Abbasi, M. Ghannad, and H. Gharooni, "Analytical Solution for Buckling Analysis of Axisymmetric Cylindrical Shell under Axial Load using Shear Deformation Theory", *Iranian Journal of Mechanical Engineering Transactions of ISME*, Vol. 26, No. 3, pp. 128-152, 2024, https://doi.org/10.30506/ijmep.2024.2009112.1948.

[35] A. H. Sofiyev, M. Avey, and N. M. Aslanova, "A Mathematical Approach to the Buckling Problem of Axially Loaded Laminated Nanocomposite Cylindrical Shells in Various Environments," *Mathematical and Computational Applications*, Vol. 30, No. 1, pp. 10, 2025, https://doi.org/10.3390/mca30010010.

[36] A. H. Nayfeh, "*Introduction to Perturbation Techniques*", New York, John Wiley & Sons, 1993.

[37] S. P. Timoshenko, and J. M. Gere, "*Theory of Elastic Stability*", 2nd, New York, Dover Publications, 2009.

Appendix 1: Dimensionless form of equilibrium equations

$$eq1:\frac{E^*h^*}{(1+\upsilon)(-1+2\upsilon)}\left[-\frac{\upsilon w^*}{R^*z^*}+\frac{h^{*2}\left(\frac{d\varphi}{dX}\right)\upsilon}{12R^*z^*}-\frac{\left(\frac{dw^*}{dX}\right)^2}{2}-V^*-\frac{h^{*2}\left(\frac{d\varphi}{dX}\right)}{12R^*z^*}+\frac{h^{*2}\left(\frac{d\psi}{dX}\right)^2\upsilon}{24}+\frac{h^{*2}\left(\frac{dw^*}{dX}\right)\left(\frac{d\psi}{dX}\right)\upsilon}{12R^*z^*}\right.$$
$$\left.+\frac{\left(\frac{dw^*}{dX}\right)^2\upsilon}{2}-\frac{\psi^2\upsilon}{2}+V^*\upsilon-\psi\upsilon-\frac{h^{*2}\left(\frac{d\psi}{dX}\right)^2}{24}-\frac{h^{*2}\left(\frac{dw^*}{dX}\right)\left(\frac{d\psi}{dX}\right)}{12R^*z^*}\right]+\varepsilon P^*h^*=0$$

$$eq2:\frac{E^*h^*}{(1+\upsilon)(-1+2\upsilon)}\left[\frac{h^{*2}\left(\frac{d^2w^*}{dX^2}\right)\left(\frac{d\psi}{dX}\right)\upsilon}{12}+\frac{h^{*2}\left(\frac{d^2\psi}{dX^2}\right)\left(\frac{dw^*}{dX}\right)\upsilon}{12}-\frac{h^{*2}\left(\frac{d^2w^*}{dX^2}\right)\left(\frac{d\psi}{dX}\right)}{12}-\frac{h^{*2}\left(\frac{d^2\psi}{dX^2}\right)\left(\frac{dw^*}{dX}\right)}{12}\right.$$
$$+\frac{h^{*2}\left(\frac{d^2\varphi}{dX^2}\right)\upsilon}{12}+\frac{h^{*4}\left(\frac{d^2\psi}{dX^2}\right)\left(\frac{d\psi}{dX}\right)}{80R^*z^*}+\frac{h^{*2}\left(\frac{d^2w^*}{dX^2}\right)\left(\frac{dw^*}{dX}\right)\upsilon}{12R^*z^*}-\frac{h^{*2}\psi\left(\frac{d\psi}{dX}\right)\upsilon}{12R^*z^*}+\frac{h^{*2}\left(\frac{dV^*}{dX}\right)\upsilon}{12R^*z^*}-h^{*2}\left(\frac{d^2\varphi}{dX^2}\right)$$
$$-\frac{h^{*2}\left(\frac{d\psi}{dX}\right)\upsilon}{6R^*z^*}-\frac{h^{*4}\left(\frac{d^2\psi}{dX^2}\right)\left(\frac{d\psi}{dX}\right)\upsilon}{80R^*z^*}-\frac{h^{*2}\left(\frac{d^2w^*}{dX^2}\right)\left(\frac{dw^*}{dX}\right)}{12R^*z^*}-\frac{h^{*2}\left(\frac{dV^*}{dX}\right)}{12R^*z^*}+\frac{h^{*2}\kappa\psi\left(\frac{d\psi}{dX}\right)}{24R^*z^*}-\frac{h^{*2}\kappa\psi\left(\frac{d\psi}{dX}\right)\upsilon}{12R^*z^*}$$
$$\left.+\frac{\kappa\psi\left(\frac{dw^*}{dX}\right)}{2}-\kappa\psi\left(\frac{dw^*}{dX}\right)\upsilon+\frac{h^{*2}\kappa\left(\frac{d\psi}{dX}\right)}{24R^*z^*}-\frac{h^{*2}\kappa\left(\frac{d\psi}{dX}\right)\upsilon}{12R^*z^*}+\frac{\kappa\left(\frac{dw^*}{dX}\right)}{2}-\kappa\left(\frac{dw^*}{dX}\right)\upsilon+\frac{\kappa\varphi}{2}-\kappa\varphi\upsilon\right]=0$$

$$eq3:\frac{E^*h^*}{(1+\nu)(-1+2\nu)}\Bigg[\frac{h^{*2}\left(\frac{d^2w^*}{dX^2}\right)\left(\frac{dw^*}{dX}\right)\left(\frac{d\psi}{dX}\right)\upsilon}{4}+\frac{h^{*2}\left(\frac{d^2w^*}{dX^2}\right)^2}{8}-\frac{h^{*2}R^*z^*\left(\frac{d^2\varphi}{dX^2}\right)\left(\frac{d\psi}{dX}\right)}{12}+\frac{h^{*2}\kappa\upsilon\left(\frac{d^2\psi}{dX^2}\right)\psi}{6}$$

$$-\frac{h^{*2}R^*z^*\left(\frac{d^2\psi}{dX^2}\right)\left(\frac{d\varphi}{dX}\right)}{12}+\frac{h^{*2}\kappa\upsilon\left(\frac{d^2\psi}{dX^2}\right)\psi^2}{12}-\frac{R^*z^*\kappa\left(\frac{d^2w^*}{dX^2}\right)}{2}-\frac{3R^*z^*\left(\frac{d^2w^*}{dX^2}\right)\left(\frac{dw^*}{dX}\right)^2}{2}-R^*z^*\left(\frac{d^2w^*}{dX^2}\right)V^*$$

$$-R^*z^*\left(\frac{dw^*}{dX}\right)\left(\frac{dV^*}{dX}\right)+\frac{h^{*2}\kappa\upsilon\left(\frac{d\psi}{dX}\right)^2\psi}{6}+\frac{R^*z^*\upsilon m_3\psi}{h^*}-\frac{R^*z^*\upsilon m_1\psi}{h^*}-\frac{R^*z^*\kappa\upsilon\left(\frac{d\varphi}{dX}\right)}{2}+2R^*z^*\kappa\upsilon\left(\frac{d^2w^*}{dX^2}\right)\psi$$

$$+R^*z^*\kappa\upsilon\left(\frac{d^2w^*}{dX^2}\right)\psi^2+\frac{h^{*2}R^*z^*\upsilon\left(\frac{d^2\psi}{dX^2}\right)\left(\frac{dw^*}{dX}\right)\left(\frac{d\psi}{dX}\right)}{4}-R^*z^*\upsilon\left(\frac{dw^*}{dX}\right)\left(\frac{d\psi}{dX}\right)\psi+2R^*z^*\kappa\upsilon\left(\frac{dw^*}{dX}\right)\left(\frac{d\psi}{dX}\right)$$

$$-R^*z^*\kappa\left(\frac{dw^*}{dX}\right)\left(\frac{d\psi}{dX}\right)\psi(X)+R^*z^*\kappa\upsilon\left(\frac{d\psi}{dX}\right)\varphi+\frac{h^{*2}R^*z^*\upsilon\left(\frac{d^2w^*}{dX^2}\right)\left(\frac{d\psi}{dX}\right)^2}{8}+\frac{h^{*2}R^*z^*\upsilon\left(\frac{d^2\varphi}{dX^2}\right)\left(\frac{d\psi}{dX}\right)}{12}$$

$$+R^*z^*\kappa\upsilon\left(\frac{d\varphi}{dX}\right)\psi-\frac{h^{*2}R^*z^*\left(\frac{d^2\psi}{dX^2}\right)\left(\frac{dw^*}{dX}\right)\left(\frac{d\psi}{dX}\right)}{4}+\frac{h^{*2}R^*z^*\upsilon\left(\frac{d^2\psi}{dX^2}\right)\left(\frac{d\varphi}{dX}\right)}{12}+\frac{3R^*z^*\upsilon\left(\frac{d^2w^*}{dX^2}\right)\left(\frac{dw^*}{dX}\right)^2}{2}$$

$$-\frac{R^*z^*\upsilon\left(\frac{d^2w^*}{dX^2}\right)\psi^2}{2}+R^*z^*\upsilon\left(\frac{d^2w^*}{dX^2}\right)V^*(X)-R^*z^*\upsilon\left(\frac{d^2w^*}{dX^2}\right)\psi-R^*z^*\kappa\left(\frac{d^2w^*}{dX^2}\right)\psi-\frac{R^*z^*\kappa\left(\frac{d^2w^*}{dX^2}\right)\psi^2}{2}$$

$$+R^*z^*\kappa\upsilon\left(\frac{d^2w^*}{dX^2}\right)-\frac{R^*z^*\kappa\left(\frac{d\psi}{dX}\right)\varphi}{2}-R^*z^*\upsilon\left(\frac{dw^*}{dX}\right)\left(\frac{d\psi}{dX}\right)+R^*z^*\upsilon\left(\frac{dw^*}{dX}\right)\left(\frac{dV^*}{dX}\right)-R^*z^*\kappa\left(\frac{dw^*}{dX}\right)\left(\frac{d\psi}{dX}\right)$$

$$+R^*z^*\kappa\upsilon\left(\frac{d\varphi}{dX}\right)-\frac{R^*z^*\kappa\left(\frac{d\varphi}{dX}\right)\psi}{2}-\frac{h^{*2}\upsilon\left(\frac{d\psi}{dX}\right)^2}{8}-\frac{\upsilon\left(\frac{dw^*}{dX}\right)^2}{2}+\frac{\upsilon\psi^2}{2}+\upsilon V^*+\frac{R^*z^*m_1\psi}{h^*}-\frac{h^{*2}\kappa\left(\frac{d^2\psi}{dX^2}\right)\psi}{12}$$

$$-\frac{R^*z^*m_3\psi}{h^*}-\upsilon\left(\frac{d^2w^*}{dX^2}\right)w^*-\frac{h^{*2}\kappa\left(\frac{d^2\psi}{dX^2}\right)\psi^2}{24}+\frac{h^{*2}\kappa\upsilon\left(\frac{d^2\psi}{dX^2}\right)}{12}+\frac{h^{*2}\upsilon\left(\frac{d^2w^*}{dX^2}\right)\left(\frac{d\varphi}{dX}\right)}{12}-\frac{h^{*2}\upsilon\left(\frac{d^2\psi}{dX^2}\right)\psi^2}{24}$$

$$+\frac{h^{*2}\upsilon\left(\frac{d^2\psi}{dX^2}\right)\left(\frac{dw^*}{dX}\right)^2}{8}-\frac{h^{*2}\left(\frac{d^2w^*}{dX^2}\right)\left(\frac{dw^*}{dX}\right)\left(\frac{d\psi}{dX}\right)}{4}+\frac{h^{*2}\upsilon\left(\frac{d^2\varphi}{dX^2}\right)\left(\frac{dw^*}{dX}\right)}{12}+\frac{3h^{*4}\upsilon\left(\frac{d^2\psi}{dX^2}\right)\left(\frac{d\psi}{dX}\right)^2}{160}-\frac{w^*m_1}{h^*}$$

$$+\frac{w^*m_3}{h^*}+\psi+\frac{h^{*2}\upsilon\left(\frac{d^2\psi}{dX^2}\right)V^*}{12}-\frac{h^{*2}\upsilon\left(\frac{d^2\psi}{dX^2}\right)\psi^2}{6}+\frac{h^{*2}\kappa\upsilon\left(\frac{d\psi}{dX}\right)^2}{6}-\frac{h^{*2}\kappa\left(\frac{d\psi}{dX}\right)^2\psi}{12}+\frac{h^{*2}\upsilon\left(\frac{d\psi}{dX}\right)\left(\frac{dV^*}{dX}\right)}{12}$$

$$-\frac{h^{*2}\upsilon\left(\frac{d\psi}{dX}\right)^2\psi}{12}-\frac{h^{*2}\left(\frac{dw}{dX}\right)^2\left(\frac{d^2\psi}{dX^2}\right)}{8}-\frac{3h^{*4}\left(\frac{d\psi}{dX}\right)^2\left(\frac{d^2\psi}{dX^2}\right)}{160}-\frac{h^{*2}\left(\frac{d\varphi}{dX}\right)\left(\frac{d^2w^*}{dX^2}\right)}{12}-\frac{h^{*2}\left(\frac{dw^*}{dX}\right)\left(\frac{d^2\varphi}{dX^2}\right)}{12}$$

$$-\frac{h^{*2}\left(\frac{d^2\psi}{dX^2}\right)V^*}{12}-\frac{h^{*2}\kappa\left(\frac{d^2\psi}{dX^2}\right)}{24}-\frac{h^{*2}\left(\frac{d\psi}{dX}\right)\left(\frac{dV^*}{dX}\right)}{12}-\frac{h^{*2}\kappa\left(\frac{d\psi}{dX}\right)^2}{12}+2R^*z^*\kappa\upsilon\left(\frac{dw^*}{dX}\right)\left(\frac{d\psi}{dX}\right)\psi+\frac{\upsilon w^*m_1}{h^*}$$

$$-\frac{\upsilon w^*m_3}{h^*}\Bigg]=0$$

$$eq4: \frac{E^* h^*}{(1+\upsilon)(-1+2\upsilon)}\Bigg[w^* + \frac{h^{*2} R^* z^* \kappa\upsilon \left(\frac{d^2\psi}{dX^2}\right)\psi^2}{12} + \frac{h^{*2} R^* z^* \upsilon \left(\frac{d^2 w^*}{dX^2}\right)\left(\frac{dw^*}{dX}\right)\left(\frac{d\psi}{dX}\right)}{4} + \frac{h^{*2} R^* z^* \kappa\upsilon \left(\frac{d^2\psi}{dX^2}\right)\psi}{6}$$

$$- R^* z^* \kappa\upsilon \left(\frac{dw^*}{dX}\right)\varphi + \frac{h^{*2} R^* z^* \kappa\upsilon \left(\frac{d\psi}{dX}\right)^2 \psi}{12} - R^* z^* \kappa\upsilon \left(\frac{dw^*}{dX}\right)^2 \psi - \frac{h^{*4} \left(\frac{d^2\psi}{dX^2}\right)\left(\frac{d\varphi}{dX}\right)}{80} - \frac{h^{*4} \left(\frac{d^2\varphi}{dX^2}\right)\left(\frac{d\psi}{dX}\right)}{80}$$

$$- \frac{3h^{*4} \left(\frac{d^2 w^*}{dX^2}\right)\left(\frac{d\psi}{dX}\right)^2}{160} - \frac{h^{*2} \kappa \left(\frac{d^2 w^*}{dX^2}\right)}{24} - \frac{h^{*2} \left(\frac{d^2 w^*}{dX^2}\right)\left(\frac{dw^*}{dX}\right)^2}{8} - \frac{h^{*2} \left(\frac{d^2 w^*}{dX^2}\right) V^*}{12} - \frac{h^{*2} \kappa \left(\frac{d\varphi}{dX}\right)}{24} + \frac{h^{*2} \upsilon \left(\frac{d\varphi}{dX}\right)}{6}$$

$$- \frac{h^{*2} \left(\frac{dw^*}{dX}\right)\left(\frac{dV^*}{dX}\right)}{12} + \frac{h^{*2} \kappa\upsilon \left(\frac{d^2 w^*}{dX^2}\right)\psi^2}{12} + \frac{h^{*2} \kappa\upsilon \left(\frac{d^2 w^*}{dX^2}\right)\psi}{6} - \frac{h^{*2} R^* z^* \left(\frac{d^2\psi}{dX^2}\right) V^*}{12} - \frac{h^{*2} R^* z^* \kappa \left(\frac{d^2\psi}{dX^2}\right)}{24}$$

$$- \frac{h^{*2} R^* z^* \left(\frac{d^2\psi}{dX^2}\right)\left(\frac{dw^*}{dX}\right)^2}{8} - \frac{h^{*2} R^* z^* \left(\frac{d^2\varphi}{dX^2}\right)\left(\frac{dw^*}{dX}\right)}{12} - \frac{h^{*2} R^* z^* \left(\frac{d^2 w^*}{dX^2}\right)\left(\frac{d\varphi}{dX}\right)}{12} - \frac{3h^{*4} R^* z^* \left(\frac{d^2\psi}{dX^2}\right)\left(\frac{d\psi}{dX}\right)^2}{160}$$

$$+ \frac{3h^{*4} \upsilon \left(\frac{d^2\psi}{dX^2}\right)\left(\frac{dw^*}{dX}\right)\left(\frac{d\psi}{dX}\right)}{80} - \frac{R^* z^* \upsilon w^* m_1}{h^*} + \frac{R^* z^* \upsilon w^* m_3}{h^*} - \frac{R^{*2} z^{*2} \upsilon\psi m_3}{h^*} + \frac{R^{*2} z^{*2} \upsilon\psi m_1}{h^*} + \frac{R^* z^* \upsilon \left(\frac{dw^*}{dX}\right)^2 \psi}{2}$$

$$- \frac{3R^* z^* \upsilon\psi^2}{2} - \frac{R^* z^* \upsilon\psi^3}{2} + \frac{R^* z^* \kappa \left(\frac{dw^*}{dX}\right)^2}{2} + \frac{h^{*2} \kappa\upsilon \left(\frac{d\varphi}{dX}\right)\psi}{12} - \frac{h^{*2} R^* z^* \upsilon \left(\frac{d\psi}{dX}\right)^2}{24} - \frac{h^{*2} R^* z^* \kappa \left(\frac{d^2\psi}{dX^2}\right)\psi^2}{24}$$

$$- \frac{h^{*2} R^* z^* \kappa \left(\frac{d\psi}{dX}\right)^2}{24} + R^* z^* \upsilon V^* - \frac{h^{*2} R^* z^* \left(\frac{d\psi}{dX}\right)\left(\frac{dV^*}{dX}\right)}{12} + \frac{h^{*2} R^* z^* \upsilon \left(\frac{d^2\psi}{dX^2}\right)\left(\frac{dw^*}{dX}\right)^2}{8} + \frac{h^{*2} R^* z^* \upsilon \left(\frac{d^2\psi}{dX^2}\right) V^*}{12}$$

$$- \frac{h^{*2} R^* z^* \upsilon \left(\frac{d^2\psi}{dX^2}\right)\psi^2}{24} - \frac{h^{*2} R^* z^* \upsilon \left(\frac{d^2\psi}{dX^2}\right)\psi}{12} - \frac{h^{*2} R^* z^* \left(\frac{dw^*}{dX}\right)\left(\frac{d^2 w^*}{dX^2}\right)\left(\frac{d\psi}{dX}\right)}{4} + \frac{h^{*2} R^* z^* \upsilon \left(\frac{dw^*}{dX}\right)\left(\frac{d^2\varphi}{dX^2}\right)\psi}{12}$$

$$+ \frac{h^{*2} R^* z^* \upsilon \left(\frac{d\varphi}{dX}\right)\left(\frac{d^2 w^*}{dX^2}\right)}{12} + \frac{3h^{*4} R^* z^* \upsilon \left(\frac{d^2\psi}{dX^2}\right)\left(\frac{d\psi}{dX}\right)^2}{160} + \frac{h^{*2} R^* z^* \kappa\upsilon \left(\frac{d^2\psi}{dX^2}\right)}{12} + \frac{h^{*2} R^* z^* \upsilon \left(\frac{d\psi}{dX}\right)\left(\frac{dV^*}{dX}\right)}{12}$$

$$-\frac{h^{*2}R^*z^*\kappa\left(\frac{d^2\psi}{dX^2}\right)\psi^2}{12}+\frac{R^*z^*\kappa\left(\frac{dw^*}{dX}\right)^2\psi}{2}+\frac{R^*z^*\kappa\left(\frac{dw^*}{dX}\right)\varphi}{2}-\frac{h^{*2}R^*z^*\kappa\left(\frac{d\psi}{dX}\right)^2\psi}{24}-\frac{h^{*2}R^*z^*\upsilon\left(\frac{d\psi}{dX}\right)^2\psi}{24}$$
$$-R^*z^*\kappa\upsilon\left(\frac{dw^*}{dX}\right)+\frac{h^{*2}R^*z^*\kappa\upsilon\left(\frac{d\psi}{dX}\right)^2\psi}{12}+\frac{R^*z^*\upsilon\left(\frac{dw^*}{dX}\right)^2\psi}{2}-\frac{3h^{*4}\left(\frac{d^2\psi}{dX^2}\right)\left(\frac{dw^*}{dX}\right)\left(\frac{d\psi}{dX}\right)}{80}-\frac{h^{*2}\upsilon\left(\frac{d^2\psi}{dX^2}\right)w^*}{12}$$
$$+\frac{h^{*2}\kappa\upsilon\left(\frac{d^2w^*}{dX^2}\right)}{12}+R^*z^*\upsilon\psi V^*+\frac{h^{*4}\upsilon\left(\frac{d^2\psi}{dX^2}\right)\left(\frac{d\varphi}{dX}\right)}{80}+\frac{h^{*2}\upsilon\left(\frac{d^2w^*}{dX^2}\right)V^*}{12}-\frac{h^{*2}\upsilon\left(\frac{d^2w^*}{dX^2}\right)\psi}{6}-\frac{h^{*2}\kappa\left(\frac{d^2w^*}{dX^2}\right)\psi^2}{24}$$
$$-\frac{h^{*2}\upsilon\left(\frac{d^2w^*}{dX^2}\right)\psi^2}{24}+\frac{3h^{*4}\upsilon\left(\frac{d^2w^*}{dX^2}\right)\left(\frac{d\psi}{dX}\right)^2}{160}+\frac{h^{*2}\upsilon\left(\frac{d^2w^*}{dX^2}\right)\left(\frac{dw^*}{dX}\right)^2}{8}+\frac{h^{*4}\upsilon\left(\frac{d^2\varphi}{dX^2}\right)\left(\frac{d\psi}{dX}\right)}{80}-\frac{h^{*2}\kappa\left(\frac{d^2w^*}{dX^2}\right)\psi}{12}$$
$$+\frac{R^*z^*w^*m_1}{h^*}-\frac{R^*z^*w^*m_3}{h^*}-\frac{R^{*2}z^{*2}\psi m_1}{h^*}+\frac{R^{*2}z^{*2}\psi m_3}{h^*}+\frac{3R^*z^*\psi^2}{2}+\upsilon w^*\psi+\frac{R^*z^*\psi^3}{2}+\frac{h^{*2}\upsilon\left(\frac{dw^*}{dX}\right)\left(\frac{dV^*}{dX}\right)}{12}$$
$$+\frac{h^{*2}\upsilon\left(\frac{d\varphi}{dX}\right)\psi}{12}-\frac{h^{*2}\kappa\left(\frac{d\varphi}{dX}\right)\psi}{24}-\frac{h^{*2}\upsilon\left(\frac{dw^*}{dX}\right)\left(\frac{d\psi}{dX}\right)}{12}+\frac{h^{*2}\kappa\upsilon\left(\frac{d\varphi}{dX}\right)}{12}\Bigg]=0$$

Appendix 2: Matrices and vectors of equilibrium equations

$$[A_0]=\begin{bmatrix}A_0[1,1] & 0 & A_0[1,3] & A_0[1,4]\\ 0 & A_0[2,2] & 0 & 0\\ A_0[3,1] & 0 & A_0[3,3] & A_0[3,4]\\ A_0[4,1] & 0 & A_0[4,3] & A_0[4,4]\end{bmatrix};\ [A_1]=\begin{bmatrix}0 & A_1[1,2] & 0 & 0\\ A_1[2,1] & 0 & A_1[2,3] & A_1[2,4]\\ 0 & A_1[3,2] & 0 & 0\\ 0 & A_1[4,2] & 0 & 0\end{bmatrix}$$

$$[A_2]=\begin{bmatrix}0 & 0 & 0 & 0\\ 0 & A_2[2,2] & 0 & 0\\ 0 & 0 & A_2[3,3] & A_2[3,4]\\ 0 & 0 & A_2[4,3] & A_2[4,4]\end{bmatrix}$$

$A_0[1,1]=E^*h^*R^*z^*(\upsilon-1)$; $A_0[1,3]=-A_0[3,1]=-E^*h^*\upsilon$; $A_0[1,4]=-A_0[4,1]=-E^*h^*R^*z^*\upsilon$;

$A_0[2,2]=\frac{E^*h^*\kappa^*R^*z^*}{2}(1-2\upsilon)$; $A_0[3,3]=E^*(m_3-m_1)(1-\upsilon)$;

$A_0[3,4]=A_0[4,3]=E^*h^*-E^*R^*z^*(m_3-m_1)(1-\upsilon)$; $A_0[4,4]=E^*R^{*2}z^{*2}(m_3-m_1)(1-\upsilon)$;

$A_1[1,2]=A_1[2,1]=-\frac{E^*h^{*3}}{12}(1-\upsilon)$; $A_1[2,3]=-A_1[3,2]=\frac{E^*h^*\kappa^*R^*z^*}{2}(1-2\upsilon)$;

$A_1[2,4]=-A_1[4,2]=\frac{E^*h^{*3}}{24}(-2\kappa^*\upsilon+\kappa^*-4\upsilon)$;

$$A_2[2,2]=\frac{E^*h^{*3}R^*z^*}{12}(\upsilon-1);\ A_2[3,3]=-\frac{E^*h^*\kappa^*R^*z^*}{2}(1-2\upsilon);\ A_2[3,4]=A_2[4,3]=-\frac{E^*h^{*3}\kappa^*}{24}(1-2\upsilon);$$

$$A_2[4,4]=-\frac{E^*h^{*3}\kappa^*R^*z^*}{24}(1-2\upsilon)$$

$$\{F_0\}=-P^*h^*R^*z^*\left(\upsilon-1+2\upsilon^2\right)\begin{Bmatrix}1\\0\\0\\0\end{Bmatrix};\ \{F_1\}=\begin{Bmatrix}F_{11}\\F_{12}\\F_{13}\\F_{14}\end{Bmatrix}$$

$$F_{11}=\frac{E^*h^*}{24}\left[(1-\upsilon)\left(2h^{*2}\left(\frac{dw_0^*}{dX}\right)\left(\frac{d\psi_0}{dX}\right)+12R^*z^*\left(\frac{dw_0^*}{dX}\right)^2+h^{*2}R^*z^*\left(\frac{d\psi_0}{dX}\right)^2\right)+12R^*z^*\upsilon{\psi_0}^2\right]$$

$$F_{12}=\frac{E^*h^*}{240}\left\{(1-\upsilon)h^{*2}\left[\left(\frac{d\psi_0}{dX}\right)\left(3h^{*2}\left(\frac{d^2\psi_0}{dX^2}\right)+20R^*z^*\left(\frac{d^2w_0^*}{dX^2}\right)\right)+20\left(\frac{dw_0^*}{dX}\right)\left(\frac{d^2w_0^*}{dX^2}\right)+20R^*z^*\left(\frac{dw_0^*}{dX}\right)\left(\frac{d^2\psi_0}{dX^2}\right)\right]\right.$$
$$\left.+10h^{*2}(2\kappa\upsilon+2\upsilon-\kappa)\psi_0\left(\frac{d\psi_0}{dX}\right)-120(1-2\upsilon)R^*z^*\kappa\psi_0\left(\frac{dw_0^*}{dX}\right)\right]$$

$$F_{13}=\frac{E^*h^*}{24}\left[24R^*z^*(1-\upsilon)V_0^*\left(\frac{d^2w_0^*}{dX^2}\right)+2h^{*2}R^*z^*(1-\upsilon)\left(\frac{d\psi_0}{dX}\right)\left(\frac{d^2\varphi_0}{dX^2}\right)+2h^{*2}R^*z^*(1-\upsilon)\left(\frac{d\varphi_0}{dX}\right)\left(\frac{d^2\psi_0}{dX^2}\right)\right.$$
$$+24R^*z^*(\upsilon+\kappa-2\kappa\upsilon)\psi_0\left(\frac{d^2w_0^*}{dX^2}\right)-2h^{*2}(2\kappa\upsilon-\kappa-2\upsilon)\psi_0\left(\frac{d^2\psi_0}{dX^2}\right)+2h^{*2}(1-\upsilon)\left(\frac{d\varphi_0}{dX}\right)\left(\frac{d^2w_0^*}{dX^2}\right)$$
$$+2h^{*2}(1-\upsilon)\left(\frac{dw_0^*}{dX}\right)\left(\frac{d^2\varphi_0}{dX^2}\right)+2h^{*2}(1-\upsilon)V_0^*\left(\frac{d^2\psi_0}{dX^2}\right)+\upsilon w_0^*\left(\frac{d^2w_0^*}{dX^2}\right)+12R^*z^*\kappa(1-2\upsilon)\psi_0\left(\frac{d\varphi_0}{dX}\right)$$
$$+24R^*z^*(1-\upsilon)\left(\frac{dw_0^*}{dX}\right)\left(\frac{dV_0^*}{dX}\right)+24R^*z^*(\kappa+\upsilon+2\kappa\upsilon)\left(\frac{dw_0^*}{dX}\right)\left(\frac{d\psi_0}{dX}\right)+12R^*z^*\kappa(1-2\upsilon)\varphi_0\left(\frac{d\psi_0}{dX}\right)$$
$$\left.+2h^{*2}(1-\upsilon)\left(\frac{d\psi_0}{dX}\right)\left(\frac{dV_0^*}{dX}\right)-12\upsilon{\psi_0}^2+12\upsilon\left(\frac{dw_0^*}{dX}\right)^2-h^{*2}(4\kappa\upsilon-2\kappa-3\upsilon)\left(\frac{d\psi_0}{dX}\right)^2\right]$$

$$F_{14}=\frac{E^*h^*}{240}\left[-240R^*z^*\upsilon\psi_0V_0^*-120R^*z^*\kappa(1-\upsilon)\varphi_0\left(\frac{dw_0^*}{dX}\right)+120R^*z^*(2\kappa-1)\upsilon\left(\frac{dw_0^*}{dX}\right)^2-120R^*z^*\kappa\left(\frac{dw_0^*}{dX}\right)^2\right.$$
$$+20h^{*2}R^*z^*(1-\upsilon)\left(\frac{d\psi_0}{dX}\right)\left(\frac{dV_0^*}{dX}\right)+20h^{*2}R^*z^*(1-\upsilon)\left(\frac{dw_0^*}{dX}\right)\left(\frac{d^2\varphi_0}{dX^2}\right)+20h^{*2}R^*z^*(1-\upsilon)V_0^*\left(\frac{d^2\psi_0}{dX^2}\right)$$
$$+20h^{*2}R^*z^*(1-\upsilon)\left(\frac{d\varphi_0}{dX}\right)\left(\frac{d^2w_0^*}{dX^2}\right)+20h^{*2}R^*z^*(\kappa+\upsilon-2\kappa\upsilon)\psi_0\left(\frac{d^2\psi_0}{dX^2}\right)-10h^{*2}R^*z^*(2\kappa-1)\upsilon\left(\frac{d\psi_0}{dX}\right)^2$$
$$-10h^{*2}(2\kappa\upsilon+2\upsilon-\kappa)\psi_0\left(\frac{d\varphi_0}{dX}\right)+20h^{*2}(1-\upsilon)V_0^*\left(\frac{d^2w_0^*}{dX^2}\right)+10h^{*2}R^*z^*\kappa\left(\frac{d\psi_0}{dX}\right)^2-480R^*z^*(1-\upsilon){\psi_0}^2$$
$$-20h^{*2}(2\kappa\upsilon-\kappa-2\upsilon)\psi_0\left(\frac{d^2w_0^*}{dX^2}\right)+20h^{*2}(1-\upsilon)\left(\frac{dw_0^*}{dX}\right)\left(\frac{dV_0^*}{dX}\right)+20h^{*2}\upsilon w_0^*\left(\frac{d^2\psi_0}{dX^2}\right)-240\upsilon\psi_0w_0^*$$
$$\left.+3h^{*4}(1-\upsilon)\left(\frac{d\varphi_0}{dX}\right)\left(\frac{d^2\psi_0}{dX^2}\right)+3h^{*4}(1-\upsilon)\left(\frac{d\psi_0}{dX}\right)\left(\frac{d^2\varphi_0}{dX^2}\right)+20h^{*2}\upsilon\left(\frac{dw_0^*}{dX}\right)\left(\frac{d\psi_0}{dX}\right)\right]$$

Appendix 3: Dimensionless form of stability equations

$$eq1:\frac{E^*h^*(\upsilon-1)}{(1+\upsilon)(-1+2\upsilon)}\left[\frac{h^{*2}}{12R^*z^*}\left(\frac{d\varphi_s}{dX^*}+\frac{dw_s^*}{dX^*}\frac{d\psi_e}{dX^*}+\frac{dw_e^*}{dX^*}\frac{d\psi_s}{dX^*}\right)+\frac{h^{*2}}{12}\left(\frac{d\psi_s}{dX^*}\right)+\frac{dw_s^*}{dX^*}\frac{dw_e^*}{dX^*}+V_s^*\right]-\frac{E^*h^*\upsilon}{(1+\upsilon)(-1+2\upsilon)}\times\left[\frac{w_s^*}{R^*z^*}+\psi_e\psi_s+\psi_s\right]$$

$$eq2:\frac{E^*h^*}{(1+\upsilon)(-1+2\upsilon)}\left[\frac{h^{*2}(\upsilon-1)}{12}\left(\frac{d^2\varphi_s}{dX^2}+\frac{dw_s^*}{dX}\frac{d^2\psi_e}{dX^2}+\frac{dw_e^*}{dX}\frac{d^2\psi_s}{dX^2}+\frac{d\psi_s}{dX}+\frac{1}{R^*z^*}\left(\frac{dw_s^*}{dX}\frac{d^2w_e^*}{dX^2}+\frac{dw_e^*}{dX}\frac{d^2w_s^*}{dX^2}\right)\right.\right.$$
$$\left.+\frac{d\psi_e}{dX}\right)-\frac{h^{*4}(\upsilon-1)}{80R^*z^*}\left(\frac{d\psi_s}{dX}+\frac{d\psi_e}{dX}\right)-\frac{h^{*2}}{24R^*z^*}\left(2\upsilon\psi_s(1+\kappa)-\kappa\psi_s\right)\frac{d\psi_e}{dX}-\frac{h^{*2}}{24R^*z^*}\left(2\upsilon\varphi_e(\kappa+1)-\kappa\psi_e\right.$$
$$\left.\left.-\kappa+4\upsilon+2\kappa\upsilon\right)\frac{d\psi_s}{dX}+\frac{h^{*2}(\upsilon-1)}{12R^*z^*}\frac{dV_s^*}{dX}+\frac{\kappa}{2}(1-2\upsilon)\psi_s\frac{dV_s^*}{dX}+\frac{\kappa}{2}(1-2\upsilon)(1+\psi_e)\frac{dw_s^*}{dX}+\frac{\kappa}{2}(1-2\upsilon)\varphi_s\right]$$

$$eq3:\frac{E^*h^*}{(1+\upsilon)(-1+2\upsilon)}\left[\frac{R^*z^*\kappa(2\upsilon-1)}{2}(1+\psi_e)\frac{d\varphi_s}{dX^*}+\frac{R^*z^*\kappa(2\upsilon-1)}{2}\psi_s\frac{d\varphi_e}{dX^*}+\frac{R^*z^*\upsilon(m_3-m_1)}{h^*}\psi_s+\psi_s+\upsilon V_s^*\right.$$
$$+\frac{(m_3-m_1)}{h^*}w_s^*+R^*z^*(\upsilon-1)\frac{dw_s^*}{dX^*}\frac{dV_e^*}{dX^*}+R^*z^*(\upsilon-1)\frac{dw_e^*}{dX^*}\frac{dv_s^*}{dX^*}+\frac{R^*z^*(m_1-m_3)}{h^*}\psi_s-\upsilon\frac{dw_e^*}{dX^*}\frac{dw_s^*}{dX^*}+\upsilon\psi_e\psi_s$$
$$-\frac{h^{*2}\kappa}{12}\left(1+\frac{\upsilon}{\kappa}-2\upsilon\right)\psi_s\left(\frac{d\psi_e}{dX^*}\right)^2+\left(\frac{h^{*2}}{3}\left(\kappa\upsilon(1+\psi_e)-\left(\frac{\kappa+\upsilon}{2}\right)\psi_e-\frac{\kappa}{2}-\frac{3\upsilon}{4}\right)\left(\frac{d\psi_s}{dX^*}\right)+\frac{h^{*2}}{12}(\upsilon-1)\left(\frac{dV_s^*}{dX^*}\right)\right.$$
$$-R^*z^*(\kappa+\upsilon+2\kappa\upsilon)\psi_s\left(\frac{dw_e^*}{dX^*}\right)-R^*z^*\left((\kappa-2\kappa\upsilon+\upsilon)+(\upsilon-2\kappa\upsilon+\kappa)\psi_e\right)\left(\frac{dw_s^*}{dX^*}\right)+\frac{R^*z^*\kappa}{2}(2\upsilon-1)\varphi_s\Big)\times$$
$$\left(\frac{d\psi_e}{dX^*}\right)+\left(\frac{h^{*2}}{12}(\upsilon-1)\left(\frac{dV_e^*}{dX^*}\right)-R^*z^*\left((\kappa-2\kappa\upsilon+\upsilon)+(\upsilon-2\kappa\upsilon+\kappa)\psi_e\right)\left(\frac{d\psi_s}{dX^*}\right)+\frac{R^*z^*\kappa}{2}(2\upsilon-1)\varphi_e\right)\times$$
$$\left(\frac{d\psi_s}{dX^*}\right)+\frac{h^{*2}}{12}(\upsilon-1)\left(\left(\frac{d\psi_s}{dX^*}\right)+\frac{1}{R^*z^*}\left(\frac{dw_s^*}{dX^*}\right)\right)\left(\frac{d^2\varphi_e}{dX^{*2}}\right)+\left(\left(\frac{h^{*2}}{12}(\upsilon-3)\right)\left(\frac{d\varphi_s}{dX^*}\right)+\left(\frac{h^{*2}R^*z^*}{4}(\upsilon-1)\right)\left(\frac{d\psi_s}{dX^*}\right)\right.$$
$$\left.+\left(\frac{h^{*2}}{4}(\upsilon-1)\right)\left(\frac{dw_s^*}{dX^*}\right)\right)\left(\frac{d\psi_e}{dX^*}\right)+\left(\frac{h^{*2}}{4}(\upsilon-1)\right)\left(\frac{dw_e^*}{dX^*}\right)\left(\frac{d\psi_s}{dX^*}\right)+\left(3R^*z^*(\upsilon-1)\right)\left(\frac{dw_s^*}{dX^*}\right)\left(\frac{dw_e^*}{dX^*}\right)-R^*z^*\times$$
$$\left(V_s^*(1-\upsilon)+(\kappa-2\kappa\upsilon+\upsilon)(\psi_s+\psi_e\psi_s)+\upsilon w_s^*\right)\left(\frac{d^2w_e^*}{dX^{*2}}\right)+\left(\frac{h^{*2}}{12}(\upsilon-1)\left(\frac{d\varphi_e}{dX^*}\right)+\frac{h^{*2}R^*z^*}{8}(\upsilon-1)\left(\frac{d\psi_e}{dX^*}\right)^2\right.$$
$$+\frac{h^{*2}}{4}(\upsilon-1)\left(\frac{dw_e^*}{dX^*}\right)\left(\frac{d\psi_e}{dX^*}\right)+\frac{3R^*z^*}{2}(\upsilon-1)\left(\frac{dw_e^*}{dX^*}\right)^2+R^*z^*\left(\kappa\upsilon\psi_e{}^2+2\kappa\upsilon\psi_e+\upsilon V_e^*+\kappa\upsilon-\kappa\psi_e-\upsilon\psi_e-V_e^*\right.$$
$$\left.-\frac{(\upsilon-\kappa)}{2}\psi_e{}^2-\frac{\kappa}{2}-\frac{\upsilon w_e^*}{R^*z^*}\right)\left(\frac{d^2w_s^*}{dX^{*2}}\right)+\frac{h^{*2}}{12}(\upsilon-1)\left(R^*z^*\left(\frac{d\psi_e}{dX^*}\right)+\left(\frac{dw_e^*}{dX^*}\right)\right)\left(\frac{d^2\varphi_s}{dX^{*2}}\right)+\left(\frac{h^{*2}R^*z^*}{12}\upsilon(\nu-1)\left(\frac{d\varphi_s}{dX^*}\right)\right.$$
$$+\left(\frac{3h^{*4}}{80}(\upsilon-1)\left(\frac{d\psi_s}{dX^*}\right)+\frac{h^{*2}R^*z^*}{4}(\upsilon-1)\left(\frac{dw_s^*}{dX^*}\right)\right)\left(\frac{d\psi_e}{dX^*}\right)+\frac{h^{*2}R^*z^*}{4}(\upsilon-1)\left(\frac{dw_e^*}{dX^*}\right)\left(\frac{d\psi_s}{dX^*}\right)+\frac{h^{*2}V_s^*}{12}(\upsilon-1)$$
$$+\frac{h^{*2}}{4}(\upsilon-1)\left(\frac{dw_s^*}{dX^*}\right)\left(\frac{dw_e^*}{dX^*}\right)-\frac{h^{*2}\psi_s}{12}(\kappa-2\kappa\upsilon+2\upsilon)(\psi_e+1)\left(\frac{d^2\psi_e}{dX^{*2}}\right)+\left(\frac{h^{*2}R^*z^*}{4}(\upsilon-1)\left(\frac{dw_e^*}{dX^*}\right)\left(\frac{d\psi_e}{dX^*}\right)\right.$$
$$+\frac{h^{*2}R^*z^*}{12}(\upsilon-1)\left(\frac{d\varphi_e}{dX^*}\right)+\frac{h^{*2}}{8}(\upsilon-1)\left(\frac{dw_e^*}{dX^*}\right)^2+\frac{3h^{*4}}{160}(\upsilon-1)\left(\frac{d\psi_e}{dX^*}\right)^2+\frac{h^{*2}}{24}\left(2\upsilon\varphi_e(2\kappa+\kappa\varphi_e-2)+2V_e^*(\upsilon-1)\right.$$
$$\left.\left.\left.-\psi_e(2\kappa+\kappa\psi_e+\upsilon\psi_e)+\kappa(2\upsilon-1)\right)\left(\frac{d^2\psi_s}{dX^{*2}}\right)+\frac{\upsilon w_s^*}{h^*}(m_1-m_3)\right]$$

$$eq4:\frac{E^*h^*}{(1+\upsilon)(-1+2\upsilon)}\Bigg[\upsilon\left(\psi_s w_e^*+\psi_e w_s^*+3R^*z^*\psi_e\psi_s+\frac{3R^*z^*{\psi_e}^2\psi_s}{2}+w_s^*\right)+\frac{h^{*2}}{24}\big(2\kappa\upsilon\psi_e+2\kappa\upsilon+2\upsilon\psi_e-\kappa\psi_e$$
$$-\kappa+4\upsilon\big)\left(\frac{d\varphi_s}{dX^*}\right)+\frac{h^{*2}}{12}(\upsilon-1)\left(\frac{dw_s^*}{dX^*}\right)\left(\frac{dV_e^*}{dX^*}\right)+\frac{h^{*2}}{12}(\upsilon-1)\left(\frac{dw_e^*}{dX^*}\right)\left(\frac{dV_s^*}{dX^*}\right)+\frac{h^{*2}R^*z^*}{24}\big(-\upsilon-\kappa+2\kappa\upsilon\big)\psi_s\times$$
$$\left(\frac{d\psi_e}{dX^*}\right)^2+R^*z^*\upsilon V_s^*+\frac{h^{*2}}{12}\left(-R^*z^*\big(\upsilon+\kappa-2\kappa\upsilon\big)\big(\psi_e+1\big)\left(\frac{d\psi_s}{dX^*}\right)+R^*z^*(\upsilon-1)\left(\frac{dV_s^*}{dX^*}\right)-\upsilon\left(\frac{dw_s^*}{dX^*}\right)\right)\left(\frac{d\psi_e}{dX^*}\right)$$
$$+\frac{h^{*2}}{12}\left(R^*z^*(\upsilon-1)\left(\frac{dV_e^*}{dX^*}\right)-\upsilon\left(\frac{dw_e^*}{dX^*}\right)\right)\left(\frac{d\psi_s}{dX^*}\right)+\frac{R^*z^*}{2h^*}\big(2\big(m_1-m_3\big)\big(w_s^*-R^*z^*\psi_s\big)-3h^*\upsilon\psi_e\psi_s\big(\psi_e+2\big)\big)$$
$$+R^*z^*\upsilon\big(\psi_eV_s^*+\psi_sV_e^*\big)+\frac{R^*z^*}{2}\big(\kappa+\upsilon-2\kappa\upsilon\big)\psi_s\left(\frac{dw_e^*}{dX^*}\right)^2+R^*z^*\big(\big(\upsilon+\kappa-2\kappa\upsilon\big)\big(1+\psi_e\big)\left(\frac{dw_s^*}{dX^*}\right)+\frac{\kappa}{2}\times$$
$$\big(1-2\upsilon\big)\varphi_s\big)\left(\frac{dw_e^*}{dX^*}\right)+\frac{\kappa R^*z^*}{2}\big(1-2\upsilon\big)\varphi_e\left(\frac{dw_s^*}{dX^*}\right)+\left(\frac{h^{*4}}{80}(\upsilon-1)\left(\frac{d\varphi_e}{dX^*}\right)+\frac{3h^{*4}R^*z^*}{160}(\upsilon-1)\left(\frac{d\psi_e}{dX^*}\right)^2+\frac{3h^{*4}}{80}\times\right.$$
$$(\upsilon-1)\left(\frac{dw_e^*}{dX^*}\right)\left(\frac{d\psi_e}{dX^*}\right)+\frac{h^{*2}R^*z^*}{8}(\upsilon-1)\left(\frac{dw_e^*}{dX^*}\right)^2-\frac{h^{*2}R^*z^*}{24}\big(\big(\kappa+\upsilon-2\kappa\upsilon\big)\big(2+\psi_e\big)\psi_e+2\big(1-\upsilon\big)V_e^*+\kappa\times$$

$$\big(1-2\upsilon\big)+\frac{2}{R^*z^*}\upsilon w_e^*\big)\left(\frac{d^2\psi_s}{dX^{*2}}\right)+\left(\frac{h^{*4}}{80}(\upsilon-1)\left(\frac{d\varphi_s}{dX^*}\right)+\left(\frac{3h^{*4}R^*z^*}{80}(\upsilon-1)\left(\frac{d\psi_s}{dX^*}\right)+\frac{3h^{*4}}{80}(\upsilon-1)\left(\frac{dw_s^*}{dX^*}\right)\right)\times\right.$$
$$\left(\frac{d\psi_e}{dX^*}\right)+\frac{3h^{*4}}{80}(\upsilon-1)\left(\frac{dw_e^*}{dX^*}\right)\left(\frac{d\psi_s}{dX^*}\right)+\frac{h^{*2}R^*z^*}{4}(\upsilon-1)\left(\frac{dw_s^*}{dX^*}\right)\left(\frac{dw_e^*}{dX^*}\right)-\frac{h^{*2}}{12}\left(\upsilon w_s^*\right)+R^*z^*\psi_s\big(\kappa+\upsilon-2\kappa\upsilon\big)\times$$
$$\big(1+\psi_e\big)+R^*z^*V_s^*\big(1-\upsilon\big)\big)\Big)\left(\frac{d^2\psi_e}{dX^{*2}}\right)+\frac{h^{*2}R^*z^*}{12}(\upsilon-1)\left(\frac{d\varphi_s}{dX^*}\right)+\left(\frac{3h^{*4}}{80}(\upsilon-1)\left(\frac{d\psi_s}{dX^*}\right)+\frac{h^{*2}R^*z^*}{4}(\upsilon-1)\left(\frac{dw_s^*}{dX^*}\right)\right)$$
$$+\frac{h^{*2}}{4}(\upsilon-1)\left(\left(R^*z^*\right)\left(\frac{dw_e^*}{dX^*}\right)\left(\frac{d\psi_s}{dX^*}\right)+\left(\frac{dw_s^*}{dX^*}\right)\left(\frac{dw_e^*}{dX^*}\right)\right)-\frac{h^{*2}}{12}\big(\big(\kappa+\upsilon-2\kappa\upsilon\big)\psi_s\big(1+\psi_e\big)-\upsilon V_s^*+V_s^*\big)+\big(\upsilon-1\big)\times$$
$$\left(\frac{h^{*4}}{80}\left(\frac{d\psi_e}{dX^*}\right)+\frac{h^{*2}R^*z^*}{12}\left(\frac{dw_e^*}{dX^*}\right)\right)\left(\frac{d^2\varphi_s}{dX^{*2}}\right)+\big(\upsilon-1\big)\left(\frac{h^{*4}}{80}\left(\frac{d\psi_s}{dX^*}\right)+\frac{h^{*2}R^*z^*}{12}\left(\frac{dw_s^*}{dX^*}\right)\right)\left(\frac{d^2\varphi_e}{dX^{*2}}\right)+\left(\frac{3h^{*4}\big(\upsilon-1\big)}{160}\times\right.$$
$$\left(\frac{d\psi_e}{dX^*}\right)^2+\frac{h^{*2}R^*z^*\big(\upsilon-1\big)}{12}\left(\frac{d\varphi_e}{dX^*}\right)+\frac{h^{*2}R^*z^*\big(\upsilon-1\big)}{4}\left(\frac{dw_e^*}{dX^*}\right)\left(\frac{d\psi_e}{dX^*}\right)+\frac{h^{*2}\big(\upsilon-1\big)}{8}\left(\frac{dw_e^*}{dX^*}\right)^2+\frac{h^{*2}}{24}\Big(\psi_e\big(\psi_e\big(2\kappa\upsilon$$
$$-\kappa-\upsilon+4\kappa\upsilon-2\kappa-4\upsilon\big)+2V_e^*\big(\upsilon-1\big)+\kappa\big(2\upsilon-1\big)\big)\Big)\left(\frac{d^2w_s^*}{dX^{*2}}\right)+\frac{R^*z^*\upsilon}{h^*}\big(m_3-\upsilon m_1\big)\big(w_s^*+R^*z^*\psi_s\big)+\frac{h^{*2}}{24}\big(2\kappa\upsilon$$
$$+2\upsilon-\kappa\big)\psi_s\left(\frac{d\varphi_e}{dX^*}\right)\Bigg]$$